Communications in Nonlinear Science and Numerical Simulation 111 (2022) 106482

Contents lists available at ScienceDirect

Communications in Nonlinear Science and Numerical Simulation

journal homepage: www.elsevier.com/locate/cnsns

Research paper

Double-zero degeneracy and heteroclinic cycles in a perturbation of the Lorenz system

A. Algaba [a], M.C. Domínguez-Moreno [a], M. Merino [a], A.J. Rodríguez-Luis [b,*]

[a] Departamento de Ciencias Integradas, Centro de Estudios Avanzados en Física, Matemática y Computación, Universidad de Huelva, 21071 Huelva, Spain

[b] Departamento de Matemática Aplicada II, E.T.S. Ingeniería, Universidad de Sevilla, Camino de los Descubrimientos s/n, 41092 Sevilla, Spain

ARTICLE INFO

Article history:
Received 17 September 2021
Received in revised form 8 March 2022
Accepted 24 March 2022
Available online 30 March 2022

Keywords:
Lorenz system
Normal form
Double-zero bifurcation
Global connections

ABSTRACT

In this paper we consider a 3D three-parameter unfolding close to the normal form of the triple-zero bifurcation exhibited by the Lorenz system. First we study analytically the double-zero degeneracy (a double-zero eigenvalue with geometric multiplicity two) and two Hopf bifurcations. We focus on the more complex case in which the double-zero degeneracy organizes several codimension-one singularities, namely transcritical, pitchfork, Hopf and heteroclinic bifurcations. The analysis of the normal form of a Hopf-transcritical bifurcation allows to obtain the expressions for the corresponding bifurcation curves. A degenerate double-zero bifurcation is also considered. The theoretical information obtained is very helpful to start a numerical study of the 3D system. Thus, the presence of degenerate heteroclinic and homoclinic orbits, T-point heteroclinic loops and chaotic attractors is detected. We find numerical evidence that, at least, four curves of codimension-two global bifurcations are related to the triple-zero degeneracy in the system analyzed.

1. Introduction

It is familiar that the dynamics exhibited by a three-dimensional autonomous system can be extremely complicated. The best known example and one of the most studied is the Lorenz system [1,2]. Although it was derived from a simple model of convection in the atmosphere, it also appears in many other fields (see, for instance, [3–11]). Due to their physical meaning, in most cases, its three parameters take positive values. However, in some situations, it also makes sense for them to be negative (see, for example, [6,7]). Therefore, it is interesting to consider that the three parameters can take any real value.

Despite the many works dedicated to knowing and explaining its extraordinarily complex dynamical behavior (for instance, we cite some of them devoted to chaotic behavior [12–18], heteroclinic loops called T-points [19–21], manifolds study [22–24], invariant algebraic surfaces [25,26] and resonances and periodic orbits [27,28]; see also references therein) there are still many aspects to be understood. Although numerical tools are essential to be able to carry out its study, the analysis of the local bifurcations of the equilibria provides valuable initial information. In this way, the full analysis of the pitchfork, Hopf and Bogdanov–Takens bifurcation exhibited by the origin of Lorenz system has already been carried out (see, for instance, [29–32]).

* Corresponding author.
E-mail address: ajrluis@us.es (A.J. Rodríguez-Luis).

https://doi.org/10.1016/j.cnsns.2022.106482

However, the study of the Hopf-pitchfork and the triple-zero degeneracies presents an additional difficulty since the origin is not an isolated equilibrium. In this case, it would be necessary to adapt the standard techniques of normal forms of the reduced system on the center manifold. This complication has encouraged us to start the study of the triple-zero bifurcation for systems invariant to the change $(x, y, z) \to (-x, -y, z)$ (symmetry exhibited by the Lorenz system), considering the corresponding normal form [33].

The triple-zero bifurcation is of codimension three when the eigenvalue has geometric multiplicity two. The study of this case, both in systems without symmetry (such as Rössler's) and in $\mathbb{Z}_2$-symmetric systems (such as Chua's) illustrates the richness and complexity of the dynamics that appears as a consequence of this degeneracy (see [34–36] and references therein). However, if the triple-zero eigenvalue has geometric multiplicity one, then the bifurcation is of codimension five [33], which reduces to codimension three if the above symmetry condition is assumed. Given the enormous difficulty of this problem, as a first step, we propose an unfolding with three parameters (see Eq. (3)). This system is of interest to us not only for small values of the parameters (on which we can do a local analysis) but also for large values (which are reached by numerical continuation). In fact, this system represents a wide family of Lorenz-like systems studied in the literature [37–42] (some of them well known, such as the Shimizu–Morioka system), although not only for small values of the parameters. Concretely, Kokubu and Roussarie demonstrate in this system the existence of non-degenerate heteroclinic cycles, which give rise to complex dynamical behaviors, in a region of the parameter space where there are small, unity order, and large parameters [42, Theorem 2.3]. We are interested in finding heteroclinic cycles in other regions of the parameter space and, in particular, to see its possible relationship with the triple-zero degeneracy.

A starting point to study the existence of heteroclinic cycles is the analysis of codimension-two local bifurcations which are close to the triple-zero. In this way, we find in the unfolding three local bifurcations of codimension two, Bogdanov–Takens (double-zero eigenvalue with geometric multiplicity one), double-zero (eigenvalue with geometric multiplicity two) and Hopf-zero. The Bogdanov–Takens bifurcation has already been analyzed [43]. The first part of this work is devoted to studying the double-zero bifurcation.

The global connections found, whose existence is guaranteed by the local analysis (Bogdanov–Takens and double-zero bifurcations), can be numerically continued, with which it is possible to study their degeneracies and their relationship with the triple-zero degeneracy (see Fig. 10). The corresponding results appear in the second part of this paper.

The final objective that we intend to achieve in this long process is the study of the triple-zero bifurcation in Lorenz-like systems obtained by perturbations of the Lorenz system, in such a way that an isolated equilibrium undergoes the triple-zero degeneracy. Thus, the Lorenz system will appear as the limit of a certain family of Lorenz-like systems (we trust that this procedure will allow to obtain interesting information about its dynamics).

The paper is organized as follows. In Section 2 we introduce the system under study and determine the local bifurcations it can exhibit, namely pitchfork, transcritical, Hopf, Bogdanov–Takens, Hopf-pitchfork, double-zero and triple-zero. The study of the double-zero degeneracy (double-zero eigenvalue with geometric multiplicity two) is carried out in Section 3. The presence of a nonlinear degeneration in the double-zero bifurcation is also discussed (some useful lemmas appear in Appendix A). Moreover, Hopf bifurcations of the nontrivial equilibria are analyzed and expressions for the loci in the parameter space where the first Lyapunov coefficient vanishes are provided (all the details appear in Appendix B). In Section 4 we conduct a numerical study starting near the double-zero bifurcation, taking advantage of the analytical results previously obtained. In this way we detect a very complex bifurcation scenario where, among other things, degenerate homoclinic and heteroclinic connections, T-point heteroclinic loops and chaotic attractors are present. We also show numerical evidence that at least four curves of codimension-two global bifurcations are related to the triple-zero degeneracy present in the unfolding analyzed. Finally, a section with conclusions is included.

2. A normal form for the Lorenz system

The Lorenz system is given by (see [1,2])

$$\begin{cases} \dot{x} = \sigma(y - x), \\ \dot{y} = \rho x - y - xz, \\ \dot{z} = -bz + xy, \end{cases} \tag{1}$$

where σ, ρ and b are real parameters. These equations are invariant under the change $(x, y, z) \to (-x, -y, z)$; therefore, the z-axis is invariant. The equilibria are the origin $(0, 0, 0)$ and, when $b(\rho - 1) > 0$, a pair of symmetric nontrivial equilibria $\left(\pm\sqrt{b(\rho-1)}, \pm\sqrt{b(\rho-1)}, \rho - 1\right)$. The origin can exhibit the following linear degeneracies:

- a pitchfork bifurcation when $\rho = 1$, $\sigma \neq 0, -1$, $b \neq 0$ [32, Sect. 3];
- a Hopf bifurcation for $\sigma = -1$, $\rho > 1$, $b \neq 0$ [30];
- a Bogdanov–Takens bifurcation when $\sigma = -1$, $\rho = 1$, $b \neq 0$ [31];
- a Hopf-pitchfork bifurcation for $\sigma = -1$, $b = 0$, $\rho > 1$;
- a triple-zero bifurcation if $\sigma = -1$, $\rho = 1$, $b = 0$.

Unfortunately the above Hopf-pitchfork and triple-zero bifurcations cannot be analyzed by the usual techniques because the origin is a non-isolated equilibrium when $b = 0$. To circumvent this obstacle in the case of the triple-zero

bifurcation, in this paper we consider a three-parameter unfolding, that is close to the normal form of the triple-zero bifurcation exhibited by the Lorenz system [33], given by

$$\begin{cases} \dot{x} = y, \\ \dot{y} = \varepsilon_1 x + \varepsilon_2 y + Axz + Byz, \\ \dot{z} = \varepsilon_3 z + Cx^2 + Dz^2, \end{cases} \tag{2}$$

where $\varepsilon_1, \varepsilon_2, \varepsilon_3 \approx 0$ and A, B, C, D are real parameters. System (2) exhibits a triple-zero bifurcation when $\varepsilon_1 = \varepsilon_2 = \varepsilon_3 = 0$. These equations are also invariant under the change $(x, y, z) \to (-x, -y, z)$.

We remark that several systems studied in the literature appear as particular cases of (2) for certain parameter choices. Thus, if $A = -1$, $C = 1$, $B = D = 0$ we obtain the Shimizu–Morioka system [37,38] (for $\varepsilon_1 = 1$, $\varepsilon_2 = -\lambda$, $\varepsilon_3 = -\alpha$) and a low-order model of magnetoconvection [39] (for $\varepsilon_1 = -\lambda$, $\varepsilon_2 = k$, $\varepsilon_3 = -1$). If $A = -a\,k$, $C = h$, $B = D = 0$, by means of the change $x = \widetilde{x}$, $y = a(\widetilde{y} - \widetilde{x})$, $z = \widetilde{z}$, a Lorenz-like system is obtained [40,41] (for $\varepsilon_1 = a\,b$, $\varepsilon_2 = -a$, $\varepsilon_3 = -c$). Finally, if $A = -1$, $C = 1$, $B = -\gamma$, $D = \delta$, $\varepsilon_1 = \tilde{A}$, $\varepsilon_2 = -1$, $\varepsilon_3 = -\beta$, the resulting system [42, Eq. (2.7)] has non-degenerate heteroclinic cycles that connect the equilibria located on the z-axis, in certain regions where ε_1 is sufficiently large, $\varepsilon_2 = -1$ and ε_3, $B < 0$ and $D > 0$ are close to zero (see [42, Theorem 2.3]).

If $A\,C \neq 0$, since system (2) is invariant to the changes

$$(x, y, z, t, \varepsilon_1, \varepsilon_2, \varepsilon_3, A, B, C, D) \longrightarrow (-x, y, -z, -t, \varepsilon_1, -\varepsilon_2, -\varepsilon_3, -A, B, C, D),$$
$$(x, y, z, t, \varepsilon_1, \varepsilon_2, \varepsilon_3, A, B, C, D) \longrightarrow (-x, y, z, -t, \varepsilon_1, -\varepsilon_2, -\varepsilon_3, A, -B, -C, -D),$$

we can take without loss of generality $A = -1$, $C = 1$

$$\begin{cases} \dot{x} = y, \\ \dot{y} = \varepsilon_1 x + \varepsilon_2 y - xz + Byz, \\ \dot{z} = \varepsilon_3 z + x^2 + Dz^2. \end{cases} \tag{3}$$

System (3) can have up to four equilibria, namely $E_1 = (0, 0, 0)$, $E_2 = (0, 0, -\varepsilon_3/D)$ if $D \neq 0$ and $E_{3,4} = \left(\pm\sqrt{-\varepsilon_1(\varepsilon_3 + D\varepsilon_1)}, 0, \varepsilon_1\right)$ if $\varepsilon_1(\varepsilon_3 + D\varepsilon_1) < 0$. Note that E_1 and E_2 are placed on the z-axis, that is an invariant set.

The Jacobian matrix of system (3) at the trivial equilibrium E_1 is

$$\begin{pmatrix} 0 & 1 & 0 \\ \varepsilon_1 & \varepsilon_2 & 0 \\ 0 & 0 & \varepsilon_3 \end{pmatrix}, \tag{4}$$

and then, its characteristic polynomial is given by $P(\lambda) = \lambda^3 + p_1\lambda^2 + p_2\lambda + p_3$, where

$$p_1 = -(\varepsilon_2 + \varepsilon_3), \quad p_2 = \varepsilon_2\varepsilon_3 - \varepsilon_1, \quad p_3 = \varepsilon_1\varepsilon_3.$$

Therefore, the origin exhibits the following bifurcations:

- a pitchfork bifurcation when $\varepsilon_1 = 0$, $\varepsilon_2 \neq 0$, $\varepsilon_3 \neq 0$. The equilibria $E_{3,4}$ appear when $\varepsilon_1(\varepsilon_3 + D\varepsilon_1) < 0$.
- A transcritical bifurcation (involving also E_2) when $\varepsilon_3 = 0$, $\varepsilon_1 \neq 0$, $\varepsilon_2 \neq 0$, $D \neq 0$.
- A Hopf bifurcation when $\varepsilon_2 = 0$, $\varepsilon_1 < 0$, $\varepsilon_3 \neq 0$.
- A Bogdanov–Takens bifurcation (a double-zero eigenvalue with geometric multiplicity one) when $\varepsilon_1 = 0$, $\varepsilon_2 = 0$, $\varepsilon_3 \neq 0$. It is of homoclinic type when $\varepsilon_3 < 0$ and of heteroclinic type if $\varepsilon_3 > 0$.
- A Hopf-zero bifurcation when $\varepsilon_2 = 0$, $\varepsilon_3 = 0$, $\varepsilon_1 < 0$.
- A double-zero bifurcation (a double-zero eigenvalue with geometric multiplicity two) when $\varepsilon_1 = 0$, $\varepsilon_3 = 0$, $\varepsilon_2 \neq 0$.
- A triple-zero bifurcation (a triple-zero eigenvalue with geometric multiplicity two) when $\varepsilon_1 = \varepsilon_2 = \varepsilon_3 = 0$.

As a first step in the study of system (3), the Bogdanov–Takens bifurcation has been analyzed in [43] whereas the double-zero bifurcation is considered in this paper. The study of the Hopf-zero and the triple-zero bifurcations will be carried out in the future.

Before starting with the study of the double-zero bifurcation, we are going to see that all the bifurcations that the equilibrium E_2 exhibits can be easily deduced from those of E_1. Indeed, to study the equilibrium $E_2 = (0, 0, -\varepsilon_3/D)$, $D \neq 0$, we translate it to the origin by means of the change

$$x = \bar{x}, \ y = \bar{y}, \ z = \bar{z} - \frac{\varepsilon_3}{D},$$

that transforms system (3) into

$$\begin{cases} \dot{\bar{x}} = \bar{y}, \\ \dot{\bar{y}} = (\varepsilon_1 + \frac{1}{D}\varepsilon_3)\bar{x} + (\varepsilon_2 - \frac{B}{D}\varepsilon_3)\bar{y} - \bar{x}\bar{z} + B\bar{y}\bar{z}, \\ \dot{\bar{z}} = -\varepsilon_3\bar{z} + \bar{x}^2 + D\bar{z}^2, \end{cases} \tag{5}$$

with $D \neq 0$.

Since system (3) is symmetric to the change

$$(x, y, z, t, \varepsilon_1, \varepsilon_2, \varepsilon_3, B, D) \longrightarrow \left(x, y, z - \frac{\varepsilon_3}{D}, t, \varepsilon_1 + \frac{\varepsilon_3}{D}, \varepsilon_2 - \frac{B\,\varepsilon_3}{D}, -\varepsilon_3, B, D\right), \tag{6}$$

it is immediate to obtain the stability and bifurcations of E_2 from the stability and bifurcations of E_1.

3. A double-zero bifurcation of the origin

The double-zero bifurcation exhibited by the equilibrium E_1 occurs when $\varepsilon_1 = 0$, $\varepsilon_3 = 0$, $\varepsilon_2 \neq 0$. Consequently, to study this codimension-two bifurcation, we fix the value of $\varepsilon_2 = \Delta^{-1} \neq 0$ (we use Δ to facilitate the writing of the expressions that will appear later) and assume that ε_1 and ε_3 are close to zero.

The results obtained in this section are summarized in the following theorem and in Fig. 1.

Theorem 3.1. *In system (3) the equilibrium E_1 exhibits a double-zero bifurcation when $\varepsilon_1 = \varepsilon_3 = 0$, $\varepsilon_2 = \Delta^{-1} \neq 0$. In a neighborhood of this codimension-two degeneracy, there are only periodic solutions (arising from a Hopf bifurcation) when $D > 0$ and $\Delta < 0$. In this case, the local codimension-one bifurcations involved are (see Fig. 1):*

(1) A transcritical bifurcation $\mathtt{T}$*, of equilibria E_1 and E_2, when $\varepsilon_3 = 0$.*
(2) Two pitchfork bifurcations $\mathtt{P}^1$*, when $\varepsilon_1 = 0$, and* $\mathtt{P}^2$*, for $\varepsilon_3 = -D\varepsilon_1 + \mathcal{O}(\varepsilon_1^2)$. They involve E_1 or E_2 and $E_{3,4}$.*
(3) A Hopf bifurcation $\mathtt{h}$ *of the equilibria $E_{3,4}$, when $\varepsilon_3 = -2D\varepsilon_1 + \mathcal{O}(\varepsilon_1^2)$, if $B \neq 2\Delta$. It is supercritical when $B > 2\Delta$ and subcritical if $B < 2\Delta$.*
(4) A heteroclinic loop between E_1 and E_2, when

$$\varepsilon_1 = -\frac{1}{2D}\,\varepsilon_3 + \frac{\Delta(B - 2\Delta)(D - \Delta)}{2D^2(2D - 3\Delta)}\,\varepsilon_3^2 + \mathcal{O}(\varepsilon_3^3), \tag{7}$$

if $B \neq 2\Delta$. It is attractive when $B > 2\Delta$ and repulsive if $B < 2\Delta$. This loop is formed by two heteroclinic connections, one is structurally stable (since it goes from E_j to E_i on the invariant z-axis) and the other one (from E_i to E_j and placed outside this axis) is more relevant as it is structurally unstable: $\mathtt{He}^{ij}$ *indicates that the connection between E_i and E_j is outside the z-axis. Concretely,* $\mathtt{He}^{21}$ *exists when $\varepsilon_3 > 0$ and* $\mathtt{He}^{12}$ *if $\varepsilon_3 < 0$.*

To study the double-zero bifurcation exhibited by the equilibrium E_1 first we apply the change of variables

$$x = Y + Z, \quad y = \varepsilon_2 Z, \quad z = X, \tag{8}$$

that transforms system (3) into

$$\begin{cases} \dot{X} = \varepsilon_3 X + (Y + Z)^2 + DX^2, \\ \dot{Y} = -\Delta\varepsilon_1 Y - \Delta\varepsilon_1 Z + \Delta XY + (\Delta - B)XZ, \\ \dot{Z} = \Delta\varepsilon_1 Y + (\Delta\varepsilon_1 + \frac{1}{\Delta})Z - \Delta XY - (\Delta - B)XZ. \end{cases} \tag{9}$$

Remark that the hyperbolic manifold of equilibrium E_1 (which is semi-hyperbolic at the double-zero) is attractive if $\Delta < 0$ and repulsive if $\Delta > 0$ (since $\dot{Z} \approx (1/\Delta)Z$). Moreover, note that system (9) is symmetric to the change $(X, Y, Z) \to (X, -Y, -Z)$, so the center manifold inherits this symmetry, that is, it will be of the form $Z = Y\Psi(X, Y^2)$, where Ψ is a smooth function. Therefore, the reduced system on the center manifold is invariant to the transformation $(X, Y) \to (X, -Y)$, so $Y = 0$ is an invariant curve of the reduced system. Consequently, it is enough to analyze the reduced system for $Y \geq 0$.

To determine the bifurcations that arise from this singularity we begin by studying the reduced system up to second order on the center manifold $Z = \Delta^2 XY + \cdots$

$$\begin{cases} \dot{X} = \varepsilon_3 X + DX^2 + Y^2 + \cdots, \\ \dot{Y} = -\Delta\varepsilon_1 Y + \Delta(1 - \Delta^2\varepsilon_1)XY + \cdots. \end{cases} \tag{10}$$

The change of variables

$$X = \frac{-1}{D}\,z - \frac{\varepsilon_3}{2D}, \quad Y = \frac{1}{\sqrt{|D|}}\,r, \quad D \neq 0, \tag{11}$$

transforms (10) into

$$\begin{cases} \dot{r} = \mu_1 r + arz, \\ \dot{z} = \mu_2 - sgn(D)r^2 - z^2, \end{cases} \tag{12}$$

where

$$\mu_1 = \frac{-\Delta}{2D}(2D\varepsilon_1 + \varepsilon_3) + \mathcal{O}(|\varepsilon_1, \varepsilon_3|^2), \quad \mu_2 = \frac{\varepsilon_3^2}{4}, \quad a = \frac{-\Delta}{D} + \mathcal{O}(|\varepsilon_1, \varepsilon_3|). \tag{13}$$

Therefore, $sgn(a) = -sgn(\Delta)sgn(D)$, i.e., $a > 0$ if $\Delta D < 0$ and $a < 0$ if $\Delta D > 0$.

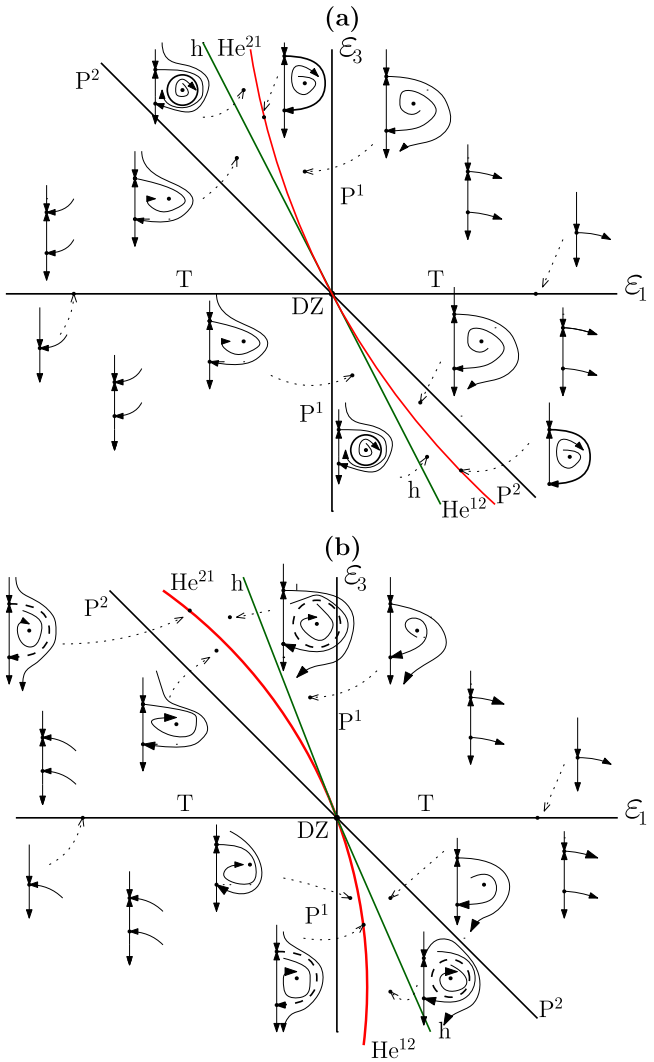

Fig. 1. Bifurcation set of system (3) in a neighborhood of the double-zero DZ exhibited by the equilibrium E_1, for $D > 0$ and $\Delta < 0$ when: (a) $B > 2\Delta$; (b) $B < 2\Delta$. The curves, according to Theorem 3.1, correspond to the following bifurcations: T, transcritical; P^1 and P^2, pitchfork; h, Hopf (supercritical when $B > 2\Delta$ and subcritical if $B < 2\Delta$); He^{12} and He^{21}, heteroclinic loop (attractive if $B > 2\Delta$ and repulsive when $B < 2\Delta$).

To study system (12) we can take advantage of the analysis of the Hopf-saddle–node degeneracy performed in [44] (we remark that (12) would correspond to a Hopf-transcritical bifurcation since $\mu_2 = \varepsilon_3^2/4$ is always positive), whose Eq. (7.4.9) is

$$\begin{cases} \dot{r} = \mu_1 r + arz, \\ \dot{z} = \mu_2 + br^2 - z^2, \end{cases} \tag{14}$$

with $b = \pm 1$. In this system there are six possible configurations (see [44, Sect.7.4] and [45, Sect.20.7]), labeled as I ($b = 1$, $a > 0$), IIa ($b = 1$, $-1 < a < 0$), IIb ($b = 1$, $a \leq -1$), III ($b = -1$, $a > 0$), IVa ($b = -1$, $-1 < a < 0$) and IVb ($b = -1$, $a < -1$). Between them, the cases of interest are IIa–IIb and III, due to the presence of periodic solutions. On the one hand, in case III, a Hopf bifurcation exists when $\mu_2 > 0$ and the periodic orbit disappears in a heteroclinic connection. On the other hand, in cases IIa–IIb, also a Hopf bifurcation exists when $\mu_2 < 0$.

Comparing (12) and (14) we see that $b = -sgn(D)$, that is, $b = +1$ if $D < 0$ and $b = -1$ if $D > 0$. Consequently, we deduce that system (12) is in case III when $D > 0$ and $\Delta < 0$. Conversely, system (12) is in cases IIa–IIb, when $D < 0$ and $\Delta < 0$. However, as $\mu_2 = \varepsilon_3^2/4 > 0$, there is no Hopf bifurcation (because, in cases IIa–IIb, it only exists when $\mu_2 < 0$). Note that the trivial cases I and IV (IVa–IVb), where only equilibria appear, occur when $D < 0$ and $\Delta > 0$ and when $D > 0$ and $\Delta > 0$, respectively.

Therefore, when $D < 0$ and $\Delta < 0$ (cases IIa–IIb), the following local bifurcations are present (see [44, Fig. 7.4.4]):

- A transcritical bifurcation when $\mu_2 = 0$, that is, when $\varepsilon_3 = 0$.
- A pitchfork bifurcation for $\mu_1^2 - a^2\mu_2 = 0$, that is, for $\varepsilon_1 = 0$ and for $\varepsilon_3 = -D\varepsilon_1 + \mathcal{O}(\varepsilon_1^2)$.

As stated above, in this case there is no Hopf bifurcation and, consequently, no heteroclinic connection.

In the rest of this section we will analyze system (12), when $D > 0$ and $\Delta < 0$ (case III), by following the steps given in [44, Sect. 7.4] for the Hopf-saddle–node bifurcation (recall that our case would correspond to a Hopf-transcritical bifurcation). The equilibria of system (12) are

$$\left(0, \pm\sqrt{\mu_2}\right) \quad \text{and} \quad \left(\pm\sqrt{\mu_2 - \frac{\mu_1^2}{a^2}}, \frac{-\mu_1}{a}\right) \quad \text{when} \quad a^2\mu_2 > \mu_1^2,$$

that in terms of the original parameters are given by

$$\left(0, \pm\frac{\varepsilon_3}{2}\right) \text{ and } \left(\pm\sqrt{\frac{-D\varepsilon_1(\varepsilon_3 + D\varepsilon_1)}{(\Delta^2\varepsilon_1 - 1)^2} + \mathcal{O}(|\varepsilon_1, \varepsilon_3|^3)}, \frac{-2D\varepsilon_1 - \varepsilon_3}{2(1 - \Delta^2\varepsilon_1)}\right), \quad \varepsilon_1(\varepsilon_3 + D\varepsilon_1) < 0.$$

Note that E_1 corresponds to the equilibrium $(0, -\varepsilon_3/2)$ and E_2 to $(0, \varepsilon_3/2)$.

From the study carried out in [44, Sect.7.4] we can deduce that the following local bifurcations are present (see Fig. 1):

- A transcritical bifurcation T of the equilibria placed on the z-axis when $\mu_2 = 0$, that is, when $\varepsilon_3 = 0$.
- A pitchfork bifurcation for $\mu_1^2 - a^2\mu_2 = 0$ that is, P^1 for $\varepsilon_1 = 0$ and P^2 for $\varepsilon_3 = -D\varepsilon_1 + \mathcal{O}(\varepsilon_1^2)$.
- A Hopf bifurcation h of the equilibria placed outside the z-axis when $\mu_1 = 0$, $\mu_2 > 0$, that is, when $\varepsilon_3 = -2D\varepsilon_1$.

However, the second-order terms are not enough to unfold neither the Hopf bifurcation nor the heteroclinic connection because, for the values of the parameter where both bifurcations appear, the system is integrable, i.e., it has an analytic first integral. In fact, for $a = 2$, it has a polynomial first integral (only case considered in [44]). Hence, it has a continuum of periodic orbits that ends in a degenerate heteroclinic connection (it corresponds to a Hopf bifurcation in which all the Lyapunov coefficients are zero, i.e., a center singular point) [44, Fig. 7.4.9]. Thus, to unfold and calculate the curves of Hopf bifurcation and heteroclinic connections (involving the two equilibria located on the z-axis), as well as their stabilities, we need the reduced system up to third order.

As the center manifold up to third order is $Z = Y(\Delta^2 X + \Delta^3 Y^2 + (D - B + 2\Delta)\Delta^3 X^2)$, we obtain the reduced system up to order three

$$\begin{cases} \dot{X} = \varepsilon_3 X + DX^2 + Y^2 + \Delta^2 XY^2, \\ \dot{Y} = -\Delta\varepsilon_1 Y + \Delta(1 - \Delta^2\varepsilon_1)XY - [\Delta - B + \Delta^2(D - B + 2\Delta)]\Delta^2 X^2 Y - \Delta^4\varepsilon_1 Y^3. \end{cases} \tag{15}$$

The change

$$X = \frac{-1}{D}z - \frac{\varepsilon_3}{2D}, \quad Y = \frac{1}{\sqrt{D - \Delta^2\varepsilon_3}}r, \tag{16}$$

transforms (15) into

$$\begin{cases} \dot{r} = \tilde{\mu}_1 r + \tilde{a}rz + \tilde{c}r^3 + \tilde{d}rz^2, \\ \dot{z} = \tilde{\mu}_2 - r^2 - z^2 + \tilde{e}r^2 z, \end{cases} \tag{17}$$

where

$$\begin{aligned} \tilde{\mu}_1 &= -\Delta\varepsilon_1 - \frac{\Delta}{2D}\varepsilon_3 + \frac{\Delta^3}{2D}\varepsilon_1\varepsilon_3 + \frac{\Delta^2(B - \Delta)}{4D^2}\varepsilon_3^2 + \mathcal{O}(|\varepsilon_1, \varepsilon_3|^3), \\ \tilde{\mu}_2 &= \frac{\varepsilon_3^2}{4} + \mathcal{O}(|\varepsilon_1, \varepsilon_3|^3), \quad \tilde{a} = \frac{-\Delta}{D} + \mathcal{O}(|\varepsilon_1, \varepsilon_3|), \quad \tilde{c} = \mathcal{O}(|\varepsilon_1, \varepsilon_3|), \\ \tilde{d} &= \frac{\Delta^2(B - \Delta)}{D^2} + \mathcal{O}(|\varepsilon_1, \varepsilon_3|), \quad \tilde{e} = \frac{2\Delta^2}{D} + \mathcal{O}(|\varepsilon_1, \varepsilon_3|). \end{aligned} \tag{18}$$

Applying Lemma A.1 of Appendix A, we obtain, modulo translation and scaling,

$$\begin{cases} \dfrac{ds}{d\tau} = \hat{\mu}_1 s + \hat{a}sw, \\ \dfrac{dw}{d\tau} = \hat{\mu}_2 - s^2 - w^2 + \hat{f}w^3, \end{cases} \tag{19}$$

where

$$\begin{aligned} \hat{\mu}_1 &= \tilde{\mu}_1 + \mathcal{O}(|\varepsilon_1, \varepsilon_3|^3), \quad \hat{\mu}_2 = \tilde{\mu}_2 + \mathcal{O}(|\varepsilon_1, \varepsilon_3|^3), \quad \hat{a} = \tilde{a} + \mathcal{O}(|\varepsilon_1, \varepsilon_3|), \\ \hat{f} &= \frac{2\Delta(B - 2\Delta)}{3D} + \mathcal{O}(|\varepsilon_1, \varepsilon_3|). \end{aligned} \tag{20}$$

Thus, in system (19), we can analyze both the Hopf bifurcation and the heteroclinic connection.

On the one hand, the Hopf bifurcation exhibits a first-order degeneracy when $B = 2\Delta$. To prove it, we obtain from system (19) the third-order reduced system

$$\begin{pmatrix} \dot{s} \\ \dot{w} \end{pmatrix} = \begin{pmatrix} 0 & -1 \\ 1 & 0 \end{pmatrix} \begin{pmatrix} s \\ w \end{pmatrix} + \begin{pmatrix} \frac{\hat{a}}{\sqrt{2\hat{a}}s_1} sw \\ -\frac{\hat{a}}{2\sqrt{2\hat{a}}s_1} s^2 - \frac{1}{\sqrt{2\hat{a}}s_1} w^2 + \frac{\tilde{f}}{\sqrt{2\hat{a}}s_1} w^3 \end{pmatrix}, \tag{21}$$

where $s_1 = \sqrt{(\hat{\mu}_2\hat{a}^3 - \hat{\mu}_1^2\hat{a} - \hat{f}\hat{\mu}_1^3)/\hat{a}^3}$. By using the recursive algorithm developed in Ref. [46], we compute the normal form of the Hopf bifurcation up to third order

$$\dot{r} = a_1 r^3 + \cdots, \quad \dot{\theta} = 1 + b_1 r^2 + \cdots, \tag{22}$$

where the first Lyapunov coefficient is given by $a_1 = 3\hat{f}/(8\sqrt{2\hat{a}}s_1)$. Therefore, the Hopf bifurcation is supercritical when $a_1 < 0$, i.e., if $\hat{f} < 0$, which occurs when $B > 2\Delta$, whereas it is subcritical if $a_1 > 0$, i.e., when $\hat{f} > 0$ or, equivalently, when $B < 2\Delta$. Consequently, a degenerate Hopf bifurcation appears when $a_1 = 0$, i.e., when $B = 2\Delta$.

On the other hand, when $\hat{f} \neq 0$, that is, if $B \neq 2\Delta$, Melnikov's method guarantees the existence of a heteroclinic connection whose curve is approximated by [47–49] (in [44] only the Hamiltonian case, $\hat{a} = 2$, is considered)

$$\mu_1 = -\frac{3\hat{a}^2\hat{f}}{2(3\hat{a}+2)}\,\mu_2 + \mathcal{O}(\mu_2^2),$$

that in terms of our parameters corresponds to

$$\varepsilon_1 = -\frac{1}{2D}\,\varepsilon_3 + \frac{\Delta(B-2\Delta)(D-\Delta)}{2D^2(2D-3\Delta)}\,\varepsilon_3^2 + \mathcal{O}(\varepsilon_3^3). \tag{23}$$

Concretely, $\mathtt{He}^{21}$ exists when $\varepsilon_3 > 0$ and $\mathtt{He}^{12}$ if $\varepsilon_3 < 0$. Note that very recently, using the nonlinear time transformation method (NTT) [50–53], the expression of the heteroclinic curve in system (19) has been computed at any order for all $\hat{a} \in \mathbb{R}$ [49, Eq.(3.20)].

With this we have completed the proof of the results stated in Theorem 3.1. Recall that all the curves mentioned in this theorem are drawn in Fig. 1.

3.1. Degenerate case $B = 2\Delta$

Next we show the steps that should be followed to study the degenerate case $B = 2\Delta$. In this situation, the Hopf bifurcation and the heteroclinic connection are not determined by system (19), and therefore we need the reduced system up to fifth order on the center manifold. Following the same steps as in the calculation up to order three, we obtain

$$\begin{cases} \dfrac{ds}{d\tau} = \hat{\mu}_1 s + \hat{a} s w + \mathcal{O}(|s,w|^4), \\ \dfrac{dw}{d\tau} = \hat{\mu}_2 - s^2 - w^2 + \mathcal{O}(|s,w|^4), \end{cases} \tag{24}$$

where $\hat{\mu}_1$, $\hat{\mu}_2$ and $\hat{a}$ are given in (20). Applying Lemmas A.2 and A.3 of Appendix A, we obtain, modulo translation and scaling,

$$\begin{cases} \dfrac{d\bar{s}}{d\tau} = \bar{\mu}_1 \bar{s} + \bar{a}\bar{s}\bar{w}, \\ \dfrac{d\bar{w}}{d\tau} = \bar{\mu}_2 - \bar{s}^2 - \bar{w}^2 + \bar{h}\bar{w}^5, \end{cases} \tag{25}$$

where

$$\bar{\mu}_1 = \hat{\mu}_1 + \mathcal{O}(|\varepsilon_1,\varepsilon_3|^3), \quad \bar{\mu}_2 = \hat{\mu}_2 + \mathcal{O}(|\varepsilon_1,\varepsilon_3|^3), \quad \bar{a} = \hat{a} + \mathcal{O}(|\varepsilon_1,\varepsilon_3|), \tag{26}$$

and the expression for $\bar{h}$ is not included because it is too long.

When $\bar{h} \neq 0$, the application of the NTT method provides the following expression for the heteroclinic curve [54]

$$\bar{\mu}_1 = -\frac{15\bar{a}^3\bar{h}}{2(3\bar{a}+2)(5\bar{a}+2)}\,\bar{\mu}_2 + \mathcal{O}(\bar{\mu}_2^2),$$

that in terms of the original parameters corresponds to

$$\varepsilon_1 = -\frac{1}{2D}\,\varepsilon_3 - \frac{15\Delta^2\bar{h}}{8D(2D-3\Delta)(2D-5\Delta)}\,\varepsilon_3^2 + \mathcal{O}(\varepsilon_3^3).$$

3.2. Hopf bifurcations of $E_{3,4}$ and E_2 in the whole $(\varepsilon_1, \varepsilon_2, \varepsilon_3)$-space

The study made so far for the Hopf bifurcation of the equilibria $E_{3,4}$ is valid when ε_1 and ε_3 are small, close to the double-zero bifurcation. In Appendix B.1 we have completed the analysis of this Hopf bifurcation for any value of ε_1 and ε_3. Specifically, we provide the value of the first Lyapunov coefficient in Eq. (B.4) and give an expression for the Hopf surface in the $(\varepsilon_1, \varepsilon_2, \varepsilon_3)$-parameter space in Eq. (B.5). These results will be useful in the numerical study of system (3) carried out in Section 4.

On the other hand, in Appendix B.2 we consider the Hopf bifurcation of the equilibrium E_2 which is related to a Bogdanov–Takens bifurcation of E_2, as we will see in Section 4. In Eq. (B.6) the value of the first Lyapunov coefficient is given.

4. Numerical study

We have seen in the previous section that the presence of a double-zero bifurcation in system (3) guarantees the existence of a heteroclinic loop which initially emerges as a planar phenomenon (in the same way that a Bogdanov–Takens bifurcation ensures the presence of homoclinic or heteroclinic connections). However, as soon as we move away from the point DZ, the heteroclinic connection will start to develop a three-dimensional structure. Thus, the numerical continuation of the heteroclinic curve away from the double-zero will make possible to determine if any point of degeneracy appears. This situation, in most cases, will imply a greater richness in the dynamics of the system.

The objective of this section is twofold. On the one hand, in Section 4.1 we are going to study the bifurcations that appear from the degenerate double-zero bifurcation ($B = 2\Delta$, where $\Delta = 1/\varepsilon_2$), completing the local information provided in Theorem 3.1 and shown in Fig. 1. On the other hand, in Section 4.2, we will find regions of the parameter space in which the system (3) exhibits a very complex dynamics.

4.1. Degenerate DZ when $B = -1$ and $D = 1$

Taking advantage of the theoretical information obtained in Section 3, we are going to carry out a numerical study of system (3) by means of the continuation software AUTO [55]. Our goal is to obtain bifurcation sets in the vicinity of the double-zero bifurcation DZ exhibited by the equilibrium $E_1 = (0, 0, 0)$ when $(\varepsilon_1, \varepsilon_3) = (0, 0)$ and $\varepsilon_2 \neq 0$. Specifically, we will take slices $\varepsilon_2 = constant$ in the $(\varepsilon_1, \varepsilon_2, \varepsilon_3)$-parameter space, fixing $B = -1$ and $D = 1$.

We know from Section 3 that the double-zero bifurcation DZ is degenerate when $\varepsilon_2 = 2/B = -2$. Then we will consider values on both sides of this singularity, for instance, $\varepsilon_2 = -1.5$ and $\varepsilon_2 = -2.5$, that correspond, respectively, to the cases $B > 2\Delta$ and $B < 2\Delta$.

4.1.1. $\varepsilon_2 = -1.5$ (case $B > 2\Delta$)

Initially, we are going to obtain the bifurcation set for $\varepsilon_2 = -1.5$. Thus, as it is usual, in order to continue numerically the bifurcation curves in a parameter plane we previously draw some bifurcation diagrams. Then, we also fix $\varepsilon_3 = -0.5$ and study the evolution of the nontrivial equilibrium $E_3 = \left(\sqrt{\varepsilon_1(0.5 - \varepsilon_1)}, 0, \varepsilon_1\right)$ versus ε_1. It exhibits a Hopf bifurcation h when $\varepsilon_1 \approx 0.2297234$. The bifurcation diagram corresponding to the asymmetric stable periodic orbit emerged from h is drawn in Fig. 2(a). This periodic orbit disappears, when $\varepsilon_1 \approx 0.2304689$, in a heteroclinic cycle He^{12} between the saddle equilibria $E_1 = (0, 0, 0)$ and $E_2 = (0, 0, 0.5)$. Recall that this loop is formed by two heteroclinic connections, one is structurally stable (since it goes from E_2 to E_1 on the invariant z-axis) and the other one is more relevant as it is structurally unstable, of codimension one (the connection from E_1 to E_2 is placed outside this axis). For this reason this heteroclinic cycle is labeled with the superscript 12, that is, He^{ij} indicates that the connection between E_i and E_j is outside the z-axis. The projection of He^{12} onto the (x, z)-plane appears in Fig. 2(c). Remark that throughout this work, with the aim of simplifying the notation, we will label the heteroclinic cycle (in fact, due to the symmetry, a pair of heteroclinic cycles exists) and the heteroclinic bifurcation with the same symbol, although they are two different objects. In addition, when necessary, we will use superscripts to indicate the equilibria that are involved in a certain bifurcation, or in a degeneration of it.

If we fix $\varepsilon_3 = -0.9$, we obtain the bifurcation diagram shown in Fig. 2(b). The periodic orbit emerged from h is of saddle type, later it becomes stable in the saddle–node bifurcation sn ($\varepsilon_1 \approx 0.397233$) and, finally, it disappears in a heteroclinic cycle He^{12} ($\varepsilon_1 \approx 0.397237$) similar to the previous case. Note that the heteroclinic loop is attractive for both values of ε_3.

Now we can numerically compute for $\varepsilon_2 = -1.5$ the loci where the bifurcations detected in Fig. 2 occur in the $(\varepsilon_1, \varepsilon_3)$-plane. Thus, in the partial bifurcation set drawn in Fig. 3(a), we can observe the curves h (Hopf bifurcation of the equilibria $E_{3,4}$), He^{12} (heteroclinic cycle between the equilibria E_1 and E_2) and sn (saddle–node bifurcation of periodic orbits). Moreover, three straight lines intersect at the double-zero point DZ, namely P^1 (pitchfork bifurcation of the origin, $\varepsilon_1 = 0$), P^2 (pitchfork bifurcation of E_2, $\varepsilon_1 = -\varepsilon_3$) and T (transcritical bifurcation between E_1 and E_2, $\varepsilon_3 = 0$). Note that in these pitchfork bifurcations the equilibria $E_{3,4}$ emerge.

Going into more detail, near the origin in the fourth quadrant the equilibria $E_{3,4}$ arise from the curve P^1 as attractive nodes (their three real eigenvalues are negative). By increasing the value of ε_1 they become attractive foci until they

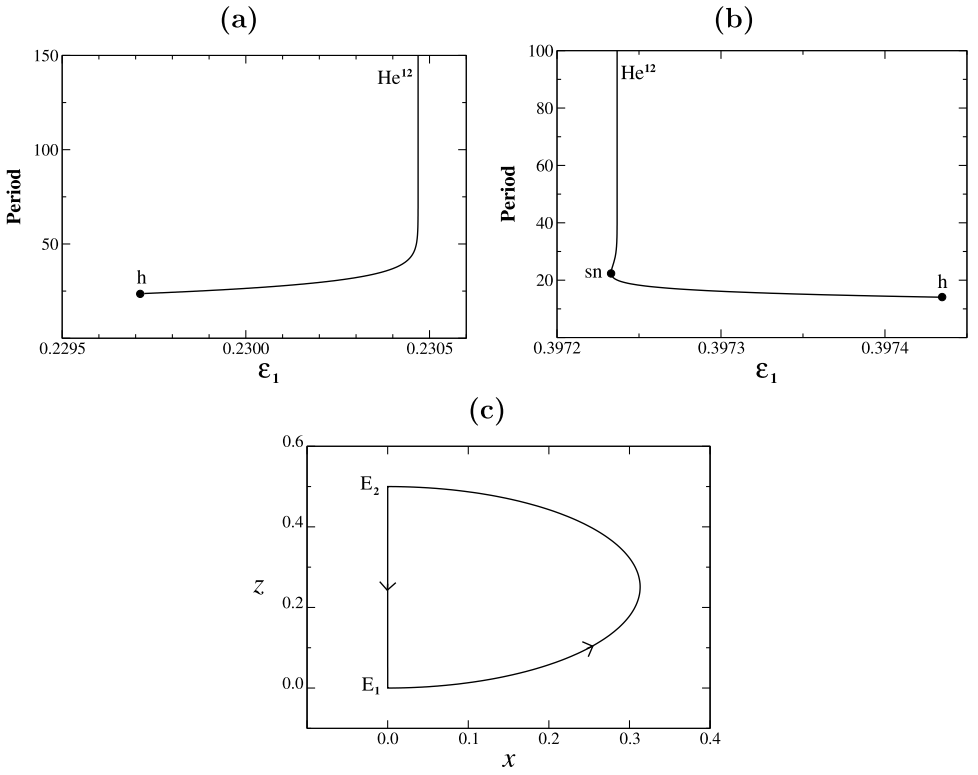

Fig. 2. For $\varepsilon_2 = -1.5, B = -1, D = 1$, bifurcation diagram of the asymmetric periodic orbit emerged from the Hopf bifurcation h, exhibited by the equilibrium E_3, when: (a) $\varepsilon_3 = -0.5$; (b) $\varepsilon_3 = -0.9$. (c) Projection onto the (x, z)-plane of the heteroclinic cycle He^{12} of panel (a) that exists when $\varepsilon_1 \approx 0.2304689$.

undergo a Hopf bifurcation h. On the other hand, in this quadrant the equilibrium E_1 is always a saddle–node ($\lambda_{1,3} < 0, \lambda_2 > 0$). This implies that, at any point in this region there exists, apart from the heteroclinic connection between E_1 and E_2, another structurally stable (codimension-zero) heteroclinic connection between the equilibria E_1 and E_3 (see Fig. 3(b) for $(\varepsilon_1, \varepsilon_3) = (0.15, -0.5)$). When the Hopf curve h is crossed, E_3 becomes a repulsive saddle-focus and then the unstable manifold of E_1 connects with the attractive periodic orbit arising from this Hopf bifurcation (see Fig. 3(c) for $(\varepsilon_1, \varepsilon_3) = (0.2304, -0.5)$). If ε_1 continues to increase, the periodic orbit grows and approaches the z-axis until the heteroclinic connection between E_1 and E_2 is formed (see Fig. 2(c)) for $(\varepsilon_1, \varepsilon_3) \approx (0.2304689, -0.5)$.

According to Eq. (B.5) of Appendix B.1, for a fixed value $\varepsilon_2 = constant$, the Hopf bifurcation curve h that emerges from the point DZ is given by the equation

$$\varepsilon_3 = \frac{3\varepsilon_1^2 - \varepsilon_2^2 + 2\varepsilon_1(1-\varepsilon_2) + \sqrt{(\varepsilon_1-\varepsilon_2)^4 + 4\varepsilon_1(\varepsilon_1^2+\varepsilon_1-\varepsilon_2^2)}}{2(-\varepsilon_1+\varepsilon_2)}.$$

In the fourth quadrant this curve is unbounded and the following inequalities hold $-2(\varepsilon_1 + 1) < \varepsilon_3 < -2\varepsilon_1$. The first one corresponds to the condition $p_2 > 0$ (a necessary condition for the existence of the Hopf bifurcation). The second inequality is due to the fact that the line $\varepsilon_3 = -2\varepsilon_1$ is an asymptote of the Hopf curve when $\varepsilon_1 \to +\infty$ and $\varepsilon_2 = constant$. Moreover, in accordance with the bifurcation diagrams of Fig. 2(a)–(b), a degenerate point Dh appears on h, when $(\varepsilon_1, \varepsilon_3) \approx (0.373821, -0.842653)$, since the first Lyapunov coefficient a_1 of the normal form vanishes (see Fig. 3(a)).

On the other hand, the curve of heteroclinic connections He^{12} is also unbounded. It emerges from the point DZ to the right of the Hopf curve h since $B > 2/\varepsilon_2$ (this agrees with the bifurcation diagram of Fig. 2(a)). However, when $(\varepsilon_1, \varepsilon_3) \approx (0.38281, -0.86445)$, both curves intersect and then, they change their relative position. Moreover, the curve He^{12} exhibits a degeneracy DHe^{12} at $(\varepsilon_1, \varepsilon_3) = (7/16, -1)$. To analyze it in the fourth quadrant of the parameter plane, we denote the eigenvalues of the Jacobian matrix at the origin E_1 as $\lambda_1, \lambda_3 < 0 < \lambda_2$, where

$$\lambda_3 = \varepsilon_3, \quad \lambda_{2,1} = \frac{\varepsilon_2 \pm \sqrt{\varepsilon_2^2 + 4\varepsilon_1}}{2},$$

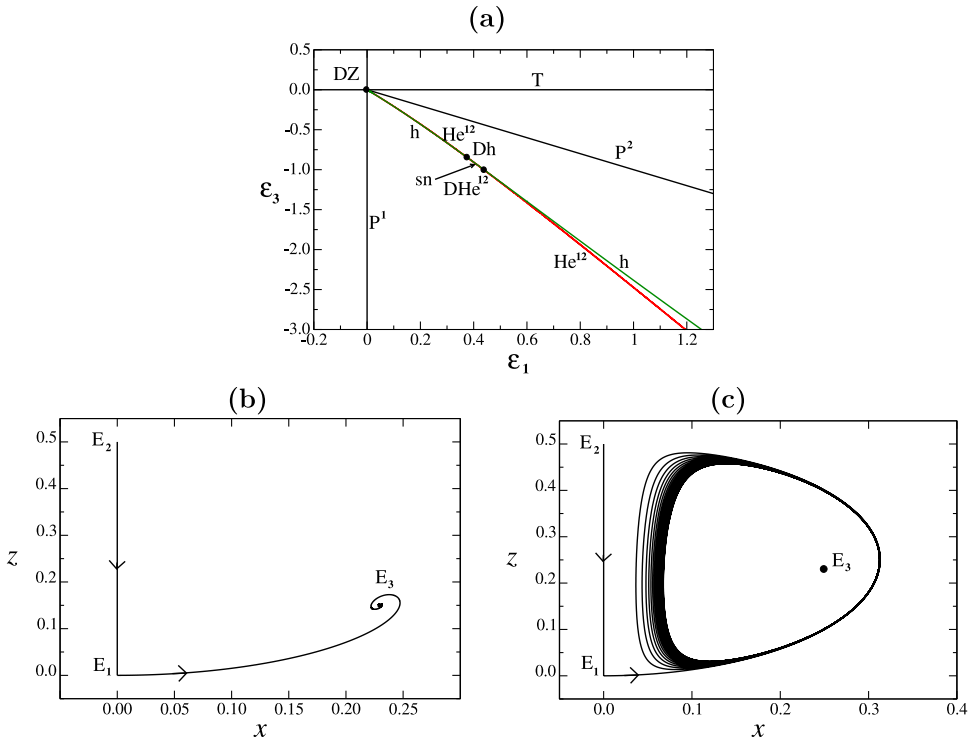

Fig. 3. For $\varepsilon_2 = -1.5, B = -1, D = 1$: (a) Partial bifurcation set in the vicinity of the double-zero point DZ, in the fourth quadrant. For $\varepsilon_3 = -0.5$, heteroclinic connections: (b) between E_2 and E_1 on the z-axis, and between E_1 and the attractive equilibrium E_3, when $\varepsilon_1 = 0.15$; (c) between E_2 and E_1 on the z-axis, and between E_1 and the stable limit cycle arising from h, when $\varepsilon_1 = 0.2304$.

and the eigenvalues of the Jacobian matrix at $E_2 = (0, 0, -\varepsilon_3)$ as $\lambda_1^* < \lambda_2^* < 0 < \lambda_3^*$, where

$$\lambda_3^* = -\varepsilon_3, \quad \lambda_{2,1}^* = \frac{\varepsilon_2 + \varepsilon_3 \pm \sqrt{(\varepsilon_2 + \varepsilon_3)^2 + 4(\varepsilon_1 + \varepsilon_3)}}{2}.$$

Now, we consider the saddle quantities $\delta_{E_1} = \left|\frac{max(\lambda_1, \lambda_3)}{\lambda_2}\right|$ and $\delta_{E_2} = \left|\frac{\lambda_2^*}{\lambda_3^*}\right|$.

Fixed a value $\varepsilon_2 = constant < 0$, in a neighborhood of the point DZ in the fourth quadrant, $\delta_{E_1} = \left|\frac{\lambda_3}{\lambda_2}\right|$, and consequently the locus where $\delta_{E_1}\delta_{E_2} = 1$ satisfies

$$\varepsilon_3 = \varepsilon_2 \frac{2\varepsilon_1 + \varepsilon_2 + \sqrt{4\varepsilon_1 + \varepsilon_2^2}}{1 - \varepsilon_1 - \varepsilon_2}.$$

Along the curve He^{12} of Fig. 3(a), and in general throughout this quadrant, both equilibria E_1 and E_2 are always real saddle.

At the degenerate point DHe^{12}, at $(\varepsilon_1, \varepsilon_3) = (7/16, -1)$,

$$\delta_{E_1}\delta_{E_2} = \left|\frac{\lambda_3\lambda_2^*}{\lambda_2\lambda_3^*}\right| = \left|\frac{-1 \cdot (-0.25)}{0.25 \cdot 1}\right| = 1,$$

in such a way that $\delta_{E_1}\delta_{E_2} > 1$ in the portion of the curve between the points DZ and DHe^{12} and, consequently, the periodic orbit involved in the heteroclinic cycle is stable (see [56,57]). On the other hand, this periodic orbit is of saddle type below DHe^{12} since $\delta_{E_1}\delta_{E_2} < 1$. We remark that the equilibrium E_1 has a double eigenvalue ($\lambda_1 = \lambda_3 = \varepsilon_3$) when $(\varepsilon_1, \varepsilon_3) \approx (0.790525, -1.913196)$. From this point $\delta_{E_1} = \left|\frac{\lambda_1}{\lambda_2}\right|$, but it is still true that $\delta_{E_1}\delta_{E_2} < 1$. Finally, as can be seen in Fig. 3(a), the degenerate points Dh and DHe^{12} are joined by the curve sn, where a saddle–node bifurcation of asymmetric periodic orbits occurs.

As the value of ε_2 increases (approaching the value $\varepsilon_2 = -2$ where the degeneration we are analyzing occurs), it is observed that the degenerate points Dh and DHe^{12}, as well as the intersection point between the curves h and

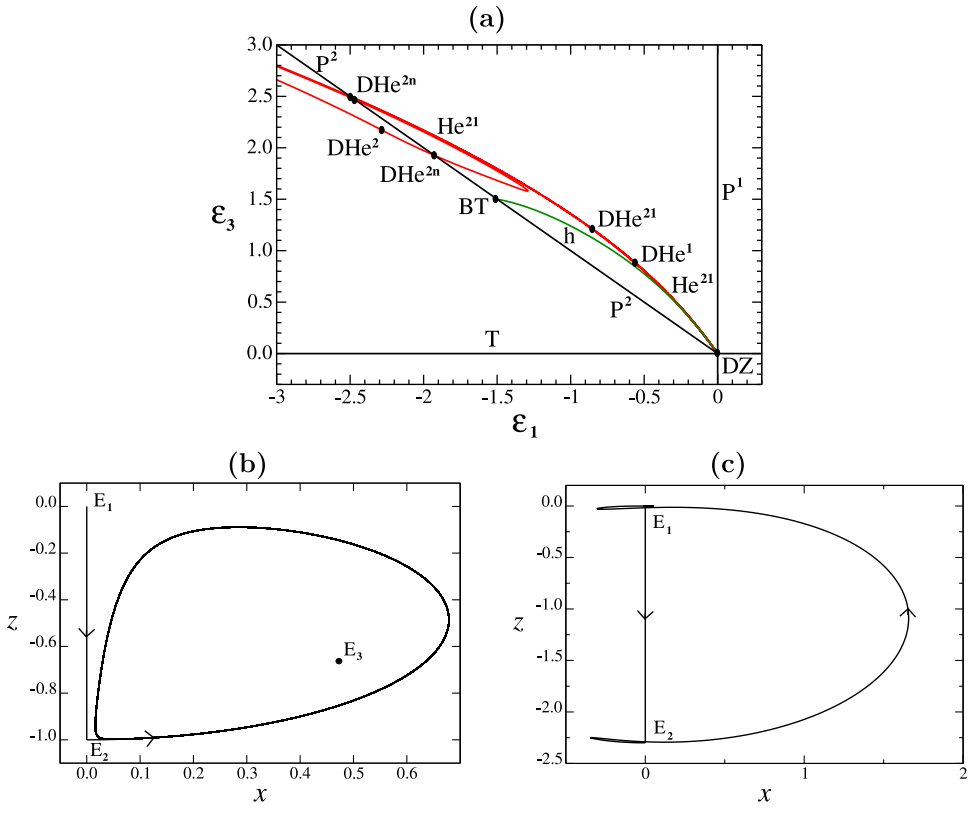

Fig. 4. For $\varepsilon_2 = -1.5, B = -1, D = 1$: (a) Partial bifurcation set, in the second quadrant, in a neighborhood of the point DZ. (b) For $\varepsilon_3 = 1$, $\varepsilon_1 = -0.663$, orbit joining the equilibrium E_2 and the periodic orbit emerged from the Hopf bifurcation h. (c) Projection onto the (x, z)-plane of the heteroclinic cycle He^{21} of panel (a) that exists when $(\varepsilon_1, \varepsilon_3) \approx (-2.4604356, 2.3)$.

He^{12}, are approaching the double-zero point DZ. Thus, for $\varepsilon_2 = -1.9$, the curve sn joins the points Dh which occurs at $(\varepsilon_1, \varepsilon_3) \approx (0.092275, -0.189040)$, and DHe^{12}, placed at $(\varepsilon_1, \varepsilon_3) = (39/400, -0.2)$. Moreover, the intersection between h and He^{12} occurs when $(\varepsilon_1, \varepsilon_3) \approx (0.09369, -0.19201)$.

According to the theoretical study done in Section 3, we know that the curves corresponding to the Hopf bifurcation of the nontrivial equilibria $E_{3,4}$ and to the heteroclinic connections between E_1 and E_2 also exist in the second quadrant of the $(\varepsilon_1, \varepsilon_3)$-plane, as can be seen in the bifurcation set for $\varepsilon_2 = -1.5$ drawn in Fig. 4(a). The Hopf bifurcation curve h is now bounded, as it ends at the point BT, which occurs at $(\varepsilon_1, \varepsilon_3) = (-1.5, 1.5)$, where the equilibrium E_2 undergoes a Bogdanov–Takens bifurcation [43]. Moreover, the curve h exists in the region $-\varepsilon_1 < \varepsilon_3 < -2\varepsilon_1$. In this case, the Hopf bifurcation is always supercritical and the attractive asymmetric periodic orbit arises to the right of the curve h. We note that the equilibria $E_{3,4}$ are attractive node when they arise from P^2. As the value of ε_1 is increased, their evolution is similar to the one mentioned above for the fourth quadrant, but exchanging the roles of E_1 and E_2 (now the unstable manifold of E_2 connects with E_3). Consequently we would have phase portraits of the same type than those of Fig. 3(b)–(c). However, the attractive periodic orbit arising from h, which in a neighborhood of the origin gives rise to the heteroclinic cycle He^{21} (the relevant heteroclinic connection, placed outside the z-axis, goes from E_2 to E_1), for other values of the parameters (for example $\varepsilon_3 = 1$), it goes approaching the equilibrium E_2 (see Fig. 4(b)) ending in a homoclinic connection to E_2 for $\varepsilon_1 \approx -0.6610023$ which will be analyzed later. We note that, in the region between the curves P^2 and He^{21} in Fig. 4(a), the eigenvalues of E_1 are $\lambda_3 = \varepsilon_3 > 0$ (whose associated eigenvector is found on the invariant axis) and $\lambda_2, \lambda_1 < 0$ (since $\varepsilon_1 < 0$), so homoclinic connections to this equilibrium cannot exist in that region.

The curve of heteroclinic cycles He^{21} also emerges from DZ and it is placed to the right of the Hopf curve h. In this case, as $\delta_{E_1}\delta_{E_2} = \left|\frac{\lambda_2\lambda_3^*}{\lambda_3\lambda_2^*}\right| > 1$, the periodic orbit involved in the heteroclinic cycle is stable.

On the curve He^{21} a first degeneracy DHe^1, placed at $(\varepsilon_1, \varepsilon_3) \approx (-0.5625, 0.8834547)$, appears when the equilibrium E_1 changes from saddle–node to saddle-focus. In the second part of this numerical study we will see the relation that exists between this degeneracy and the homoclinic connection to E_2 (originated by the periodic orbit drawn in Fig. 4(b)).

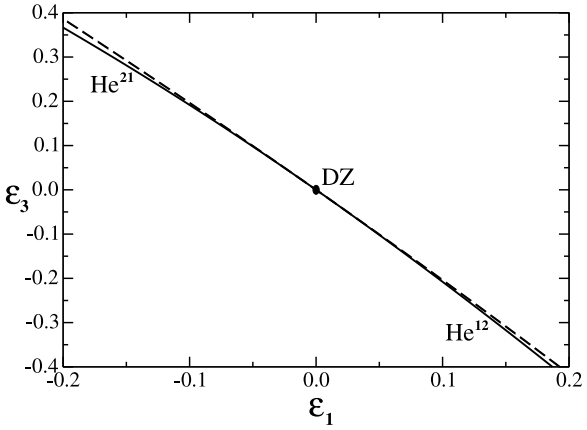

Fig. 5. For $B = -1$, $D = 1$ and $\varepsilon_2 = -1.5$, comparison between numerical continuation (solid) and analytical first-order approximation given by (23) (dashed) for the heteroclinic bifurcation curves $\mathtt{He}^{12}$ and $\mathtt{He}^{21}$.

There is also a degenerate point $\mathtt{DHe}^{21}$, located at $(\varepsilon_1, \varepsilon_3) \approx (-0.853422, 1.210866)$, similar to that found in the fourth quadrant, where $\delta_{E_1}\delta_{E_2} = 1$, condition that occurs when

$$\varepsilon_1 = -\varepsilon_3 \left(1 + 2\varepsilon_2 \left(\frac{\varepsilon_2 + \varepsilon_3}{\varepsilon_2 + 2\varepsilon_3}\right)^2\right),$$

since now $\delta_{E_1}\delta_{E_2} = \left|\frac{Re(\lambda_2)\lambda_1^*}{\lambda_3\lambda_2^*}\right|$. From this point $\mathtt{DHe}^{21}$, $\delta_{E_1}\delta_{E_2} < 1$.

Unlike what happens with the degeneracy of the same type located in the fourth quadrant, the point $\mathtt{DHe}^{21}$ that exists in the second quadrant is not related to the degeneration exhibited by the double-zero bifurcation DZ at the point DDZ, which occurs at $(\varepsilon_1, \varepsilon_2, \varepsilon_3) = (0, -2, 0)$. Indeed, when we vary the parameter ε_2 approaching the value where the degeneration DDZ occurs, the point $\mathtt{DHe}^{21}$ moves away from the point DZ, and specifically, for $\varepsilon_2 = -2$, we obtain $\mathtt{DHe}^{21}$, located at $(\varepsilon_1, \varepsilon_3) \approx (-1.15082, 1.64582)$.

Subsequently the curve of heteroclinic connections $\mathtt{He}^{21}$ intersects with the line $\mathtt{P}^2$ at the point $\mathtt{DHe}^{2n}$, which occurs at $(\varepsilon_1, \varepsilon_3) \approx (-2.5007629, 2.5007629)$, where the equilibrium E_2 has a zero eigenvalue $\lambda_1^* = 0$ and, as a consequence, E_2 has a two-dimensional unstable manifold when crossing the line $\mathtt{P}^2$. Later, the curve $\mathtt{He}^{21}$ has a turning point outside the range of Fig. 4(a), for $(-10.761538, 5.917409)$, and cuts again $\mathtt{P}^2$ at $\mathtt{DHe}^{2n}$, placed at $(\varepsilon_1, \varepsilon_3) \approx (-2.4692096, -2.4692096)$. As $\mathtt{He}^{21}$ approaches the Bogdanov–Takens point BT, it experiences a new turning point and thus it intersects a third time with $\mathtt{P}^2$ at $\mathtt{DHe}^{2n}$, which occurs at $(\varepsilon_1, \varepsilon_3) \approx (-1.9246322, -1.9246322)$. In the region of the parameter plane where E_2 has a two-dimensional unstable manifold, a new degeneration $\mathtt{DHe}^2$ appears on the heteroclinic cycle, for $(\varepsilon_1, \varepsilon_3) \approx (-2.285538, 2.1724805)$, because E_2 goes from real saddle to saddle focus when crossing this point. As can be seen in Fig. 4(c), for $(\varepsilon_1, \varepsilon_3) \approx (-2.4604356, 2.3)$, the equilibrium E_1 is a saddle-focus (with a two-dimensional stable manifold). We remark that bifurcations of generic heteroclinic loops (between a saddle–node hyperbolic equilibrium and a non-hyperbolic equilibrium which undergoes a pitchfork bifurcation) are considered in [58] for a four-dimensional system. In our case the hyperbolic equilibrium E_1 is a saddle-focus at the points $\mathtt{DHe}^{2n}$.

We conclude our study for $\varepsilon_2 = -1.5$ showing, for the heteroclinic curves $\mathtt{He}^{12}$ and $\mathtt{He}^{21}$, the good agreement between the theoretical prediction given by Eq. (23) and the numerical results, in the vicinity of the double-zero degeneracy (see Fig. 5).

4.1.2. $\varepsilon_2 = -2.5$ (case $B < 2\Delta$)

Next we set $\varepsilon_2 = -2.5$, on the other side of the value where the degeneracy DDZ occurs, and we find partial bifurcation sets in the fourth and second quadrants of the $(\varepsilon_1, \varepsilon_3)$-parameter plane. In this way we see in Fig. 6(a) the same bifurcation curves, related to double-zero bifurcation DZ, which are present in Fig. 3(a) except the curve of saddle–node bifurcation of periodic orbits sn. This is because no point of degeneration appears on the curves h (Hopf of the nontrivial equilibria $E_{3,4}$) and $\mathtt{He}^{12}$ (heteroclinic cycle) and then, the saddle periodic orbit arisen from h ends at the heteroclinic loop $\mathtt{He}^{12}$ (it holds $\delta_{E_1}\delta_{E_2} = \left|\frac{\lambda_3\lambda_2^*}{\lambda_2\lambda_3^*}\right| < 1$). We remark that the relative position between the curves h and $\mathtt{He}^{12}$ have changed in the vicinity of the point DZ, with respect to what they had in Fig. 3(a) when $\varepsilon_2 = -1.5$ (now we are in the case $B < 2/\varepsilon_2$). In the entire fourth quadrant, as was the case for $\varepsilon_2 = -1.5$, both equilibria E_1 and E_2 are always real saddle.

In Fig. 6(b), for $\varepsilon_2 = -2.5$, we see a partial bifurcation set in the second quadrant, with the curves related to the double-zero bifurcation DZ. As in the case of $\varepsilon_2 = -1.5$, the curve of Hopf bifurcation h ends at a Bogdanov–Takens bifurcation BT exhibited by the equilibrium E_2, which occurs at $(\varepsilon_1, \varepsilon_3) = (-2.5, 2.5)$. Initially, in accordance with the theoretical analysis

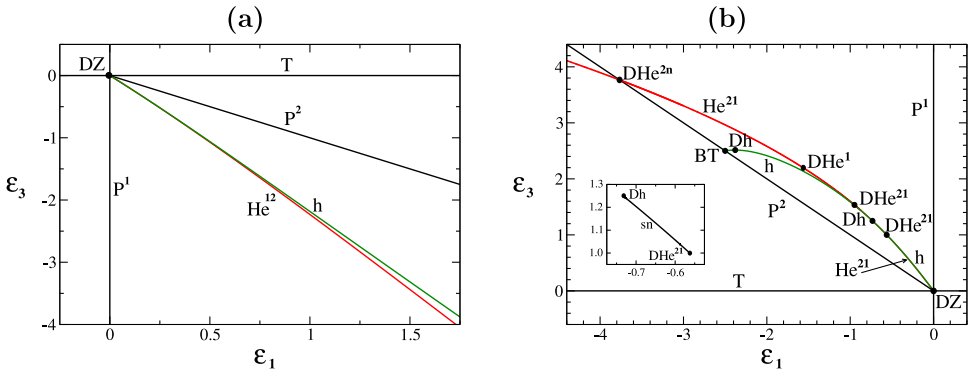

Fig. 6. For $\varepsilon_2 = -2.5, B = -1, D = 1$, partial bifurcation set in a neighborhood of the point DZ: (a) in the fourth quadrant; (b) in the second quadrant.

of Section 3, h arises from the point DZ to the right of the curve He^{21} (both curves are related by a non-stable periodic orbit). Subsequently h and He^{21} intersect and moreover at the point Dh, located at $(\varepsilon_1, \varepsilon_3) \approx (-0.732961, 1.24975)$, the first Lyapunov coefficient vanishes, in such a way that a stable periodic orbit emerges above this point. The curve of saddle–node bifurcations of periodic orbits sn, arisen from this degeneracy, is drawn in the inset of Fig. 6(b).

As in the fourth quadrant, in a neighborhood of the point DZ, it holds $\delta_{E_1}\delta_{E_2} = \left|\frac{\lambda_2\lambda_3^*}{\lambda_3\lambda_2^*}\right| < 1$ on the heteroclinic curve He^{21}. Later, a degeneracy DHe^{21}, where $\delta_{E_1}\delta_{E_2} = \left|\frac{-0.25\cdot(-1)}{1\cdot 0.25}\right| = 1$, occurs at $(\varepsilon_1, \varepsilon_3) = (-9/16, 1)$. This point is the end of the curve sn drawn in Fig. 6(b). We note that the existence in the second quadrant of the degeneration points Dh and DHe^{21} is due to the symmetry exhibited by system (3). Indeed, starting from the values of the degeneracy DHe^{12} for $\varepsilon_2 = -1.5$ in the fourth quadrant, and using the Eqs. (6), the values of the first degeneracy DHe^{21} in the second quadrant are obtained for $\varepsilon_2 = -2.5$. In particular, the eigenvalues of the equilibrium E_1 become those of the equilibrium E_2 and vice versa. On the other hand, the symmetrical point to Dh in the fourth quadrant for $\varepsilon_2 = -1.5$ appears in the plane $\varepsilon_2 \approx -2.342652$ for $(\varepsilon_1, \varepsilon_3) \approx (-0.468831, 0.842652)$. Logically the points on the line T, for $\varepsilon_3 = 0$, remain invariant under this symmetry, in particular the point DZ and its degeneracies.

On the Hopf curve h, near the point BT, there is a second degeneration point Dh, located at $(\varepsilon_1, \varepsilon_3) \approx (-2.37898, 2.51397)$, where the first Lyapunov coefficient vanishes. This new point arises from the bifurcation BT when $\varepsilon_2 = -2$, and it is related with a codimension-three Bogdanov–Takens bifurcation [43]. Analogously, on the curve of heteroclinic connections He^{21} there is a second degeneration point DHe^{21}, which occurs at $(\varepsilon_1, \varepsilon_3) \approx (-0.94877, 1.53434)$, where $\delta_{E_1}\delta_{E_2} = \left|\frac{\lambda_2\lambda_1^*}{\lambda_3\lambda_2^*}\right| = 1$. Once that point is passed, it holds $\delta_{E_1}\delta_{E_2} < 1$.

In this area is now located the degeneration DHe^{1} at $(\varepsilon_1, \varepsilon_3) \approx (-1.5625, 2.1968639)$ (see Fig. 6(b)) unlike what happened for $\varepsilon_2 = -1.5$, since at that point $\delta_{E_1}\delta_{E_2} > 1$ (see Fig. 4(a)). Subsequently the curve He^{21} intersects with the line P^2 at the point DHe^{2n}, situated at $(\varepsilon_1, \varepsilon_3) \approx (-3.7663574, -3.7663574)$, where E_2 has a zero eigenvalue, so that E_2 has a two-dimensional unstable manifold when crossing P^2.

4.1.3. Codimension-two bifurcations around the degenerate DZ

Next, we are going to study in the three-parameter space the loci where the detected codimension-two bifurcations occur. In Fig. 7(a) and (b) we represent, in a neighborhood of the point DDZ, which occurs at $(\varepsilon_1, \varepsilon_2, \varepsilon_3) = (0, -2, 0)$, the projections of the curves Dh, DHe^{12} and DHe^{21} onto the planes $(\varepsilon_2, \varepsilon_1)$ and $(\varepsilon_2, \varepsilon_3)$, respectively. We have also included the curve $\mathrm{He}^{\mathrm{DE1}}$ ($\mathrm{He}^{\mathrm{DE2}}$), where the equilibrium E_1 (E_2) has a non-leading double eigenvalue at the heteroclinic cycle He^{12} (He^{21}).

As can be seen, the curve DHe^{12} (as is the case with curve Dh) arises from the degeneracy DDZ, exhibited by the double-zero bifurcation DZ and analyzed in this paper for system (3). Moreover, DHe^{12} intersects with the curve $\mathrm{He}^{\mathrm{DE1}}$ when $(\varepsilon_1, \varepsilon_2, \varepsilon_3) = (0.64, -1.2, -1.6)$. At this point, the eigenvalues of E_1 are $\lambda_1 = \lambda_3 = -1.6, \lambda_2 = 0.4$ and those of E_2 are $\lambda_1^* = -2.4, \lambda_2^* = -0.4, \lambda_3^* = 1.6$, so that $\delta_{E_1}\delta_{E_2} = 1$. Because of the symmetry exhibited by system (3), the same situation appears for $(\varepsilon_1, \varepsilon_2, \varepsilon_3) = (-0.96, -2.8, 1.6)$, interchanging the roles of the equilibria E_1 and E_2. We note that there is no degeneration DHe^{21} on the surface He^{21} for $\varepsilon_2 < -2.8$, but there is degeneration DHe^{12} for $\varepsilon_2 > -1.2$ to the right of the curve $\mathrm{He}^{\mathrm{DE1}}$.

4.2. Looking for more complex behavior ($B = -0.1, D = 0.01, \varepsilon_2 = -1$)

Our next objective is to analyze some of the degenerations detected on the curves He^{12} and He^{21}, although now we will take $\varepsilon_2 = -1$, $B = -0.1$ and $D = 0.01$. Thus, for the same value of ε_2, we will find degenerations of the type DHe^{2}

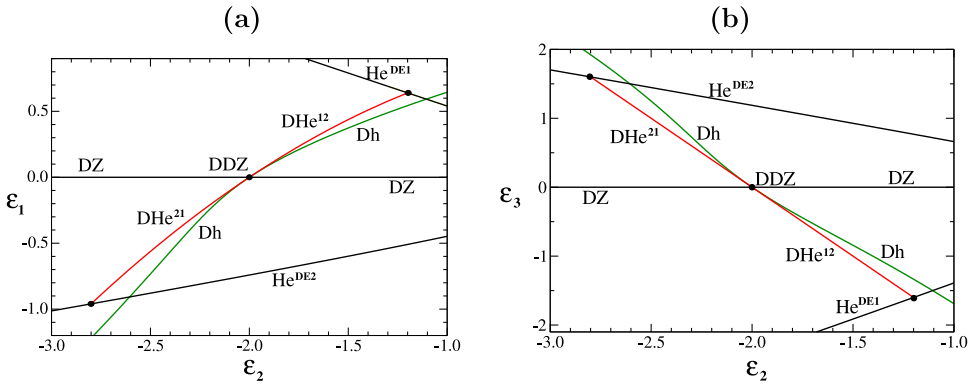

Fig. 7. For $B = -1, D = 1$, projection in the vicinity of the codimension-three bifurcation DDZ of the curves Dh (degenerate Hopf bifurcation of the equilibria $E_{3,4}$), DHe^{12} and DHe^{21} (degeneracy condition $\delta_{E_1}\delta_{E_2} = 1$ on the curves of heteroclinic connections He^{12} and He^{21}, respectively), $\mathrm{He}^{\mathrm{DE1}}$ and $\mathrm{He}^{\mathrm{DE2}}$ (non-leading double eigenvalue of E_1 on He^{12} and of E_2 on He^{21}, respectively) onto: (a) the $(\varepsilon_2, \varepsilon_1)$-plane. (b) the $(\varepsilon_2, \varepsilon_3)$-plane.

and DHe^1 in the fourth and second quadrants, respectively. This situation was not possible with the previous values of the parameters. These degeneracies will allow us to find regions in which there are complex dynamical behaviors.

On the one hand, in the partial bifurcation set of Fig. 8(a)–(b) we see that the curve of nondegenerate heteroclinic cycles He^{12} arises from the double-zero degeneracy DZ. Initially, these heteroclinic cycles are attractive ($\delta_{E_1}\delta_{E_2} > 1$) but their stability changes when crossing the points DHe^{12}. In the fourth quadrant we have found two of these points DHe^{12}, placed at $(\varepsilon_1, \varepsilon_3) \approx (1.057329, -0.028677)$ and $(\varepsilon_1, \varepsilon_3) \approx (17.952116, -0.653279)$, where $\delta_{E_1}\delta_{E_2} = \left|\frac{\lambda_3 Re(\lambda_2^*)}{\lambda_2 \lambda_3^*}\right| = 1$ (in fact, $\delta_{E_1}\delta_{E_2} < 1$ at the points on the curve He^{12} between both of them). Specifically, the eigenvalues of E_2, in terms of the parameters B and D, are given by

$$\lambda_3^* = -\varepsilon_3, \quad \lambda_{2,1}^* = \frac{\varepsilon_2 - \frac{B}{D}\varepsilon_3 \pm \sqrt{\left(\varepsilon_2 - \frac{B}{D}\varepsilon_3\right)^2 + 4\left(\varepsilon_1 + \frac{\varepsilon_3}{D}\right)}}{2}.$$

Thus, the curve where the equilibrium E_2 changes from real saddle to saddle-focus intersects the curve He^{12} in two points. Indeed, when $\varepsilon_1 > 0$, the equilibrium E_1 is always a real saddle along the curve He^{12}. For its part, E_2 is also a real saddle when it arises from DZ, but it becomes a saddle-focus from the point DHe^2, which occurs at $(\varepsilon_1, \varepsilon_3) \approx (0.2328879, -0.00508985)$, placed between DZ and the first degeneracy DHe^{12} (see Fig. 8(b)). Below the second degeneration DHe^{12} there is another similar point DHe^2, situated at $(\varepsilon_1, \varepsilon_3) \approx (72.3710927, -2.7397356)$, where E_2 goes from saddle-focus to real saddle (see Fig. 8(a)).

Several bifurcation curves emerge from the first of these degenerate points DHe^2. Specifically, in Fig. 8(b) we have drawn two curves of homoclinic connections to the origin, H_1^1 and H_2^1, fulfilling that $\delta_{E1} < 1$ when they arise from DHe^2. These curves H_1^1 and H_2^1 end in other degenerations that exist on He^{12} for the values $(\varepsilon_1, \varepsilon_3) \approx (90, -3.4225563)$ and $(\varepsilon_1, \varepsilon_3) \approx (75.0355, -2.8429)$, respectively.

On the homoclinic curve H_1^1 there is a degenerate point DH_1^1, which occurs at $(\varepsilon_1, \varepsilon_3) \approx (1.1370815, -0.6777442)$, where $\delta_{E_1} = 1$, because its eigenvalues fulfill $\lambda_1 < \lambda_3 = -\lambda_2$. In Fig. 8(b) we also find two curves sn and SN of saddle–node bifurcations of (asymmetric and symmetric, respectively) periodic orbits. Whereas sn exists between this point and the degeneration DHe^2 closest to DZ, the curve SN connects this DHe^2 point with $(\varepsilon_1, \varepsilon_3) \approx (75.0355, -2.8429)$, point where the curve H_2^1 ends on He^{12}.

These curves (H_1^1, sn, SN, H_2^1, ...) are the first of an infinite sequence of curves of the same type (homoclinic connections to E_1, saddle–node bifurcations of asymmetric and symmetric periodic orbits, ...) that all arise from the degeneracy DHe^2. Curves of period-doubling bifurcations (exhibited by the asymmetric periodic orbits involved in sn) and of symmetry-breaking bifurcations (exhibited by the symmetric periodic orbits involved in SN) are also present. As a consequence of the above, in the region between the aforementioned bifurcation curves and He^{12}, we can find attractors of various types as shown in Fig. 8(c)–(f).

On the other hand, in the second quadrant (see Fig. 9(a)) there is a single point DHe^{21} (similar to that found in the second quadrant in Fig. 4(a)), which occurs at $(\varepsilon_1, \varepsilon_3) \approx (-1.11049, 0.01772)$, where $\delta_{E_1}\delta_{E_2} = \left|\frac{Re(\lambda_2)\lambda_3^*}{\lambda_3 \lambda_2^*}\right| = 1$. In the rest of the curve He^{21} (starting from the point DHe^{21}), it is true that $\delta_{E_1}\delta_{E_2} < 1$. Remark that these degeneracies DHe^{21}, in which one of the two equilibria E_1 and E_2 involved in the heteroclinic cycle is saddle-focus, are not related to the codimension-three degeneracy DDZ previously analyzed. In this quadrant, the Hopf bifurcation of the equilibria $E_{3,4}$ is always supercritical and the curve h is bounded as it joins the points DZ and BT, placed at $(\varepsilon_1, \varepsilon_3) = (-10, 0.1)$ (where E_2 exhibits a Bogdanov–Takens bifurcation). Since $\varepsilon_3 > 0$, this Bogdanov–Takens bifurcation is of homoclinic type [43]. Consequently, apart from other bifurcation curves, a curve H_1^2 of homoclinic connections to E_2 emerges from BT (see Fig. 9(b)–(c)).

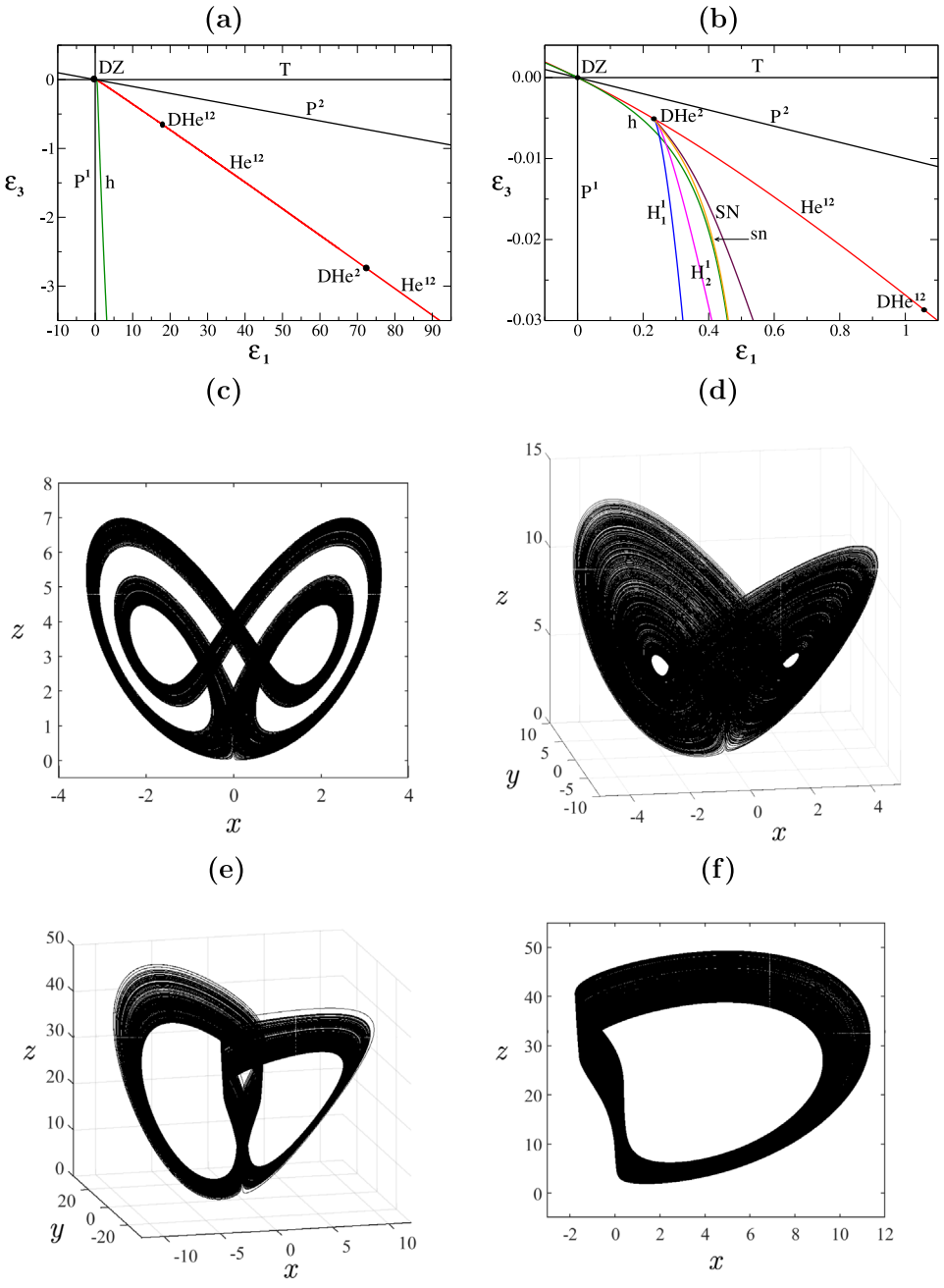

Fig. 8. For $\varepsilon_2 = -1, B = -0.1, D = 0.01$: (a) partial bifurcation set in the fourth quadrant; (b) zoom of panel (a) in a neighborhood of the point DZ. For $\varepsilon_3 = -1$ geometric Lorenz attractor when: (c) $\varepsilon_1 = 3$ with initial conditions $(x_0, y_0, z_0) = (3, -2, 6.5)$. (d) $\varepsilon_1 = 5$ with initial conditions $(x_0, y_0, z_0) = (2.8, 1, 5)$. (e) $\varepsilon_1 = 15$ with initial conditions $(x_0, y_0, z_0) = (0.2, 0.3, 20)$. (f) $\varepsilon_1 = 16.3$ with initial conditions $(x_0, y_0, z_0) = (-0.2, 1.2, 17)$.

When $\varepsilon_1 < 0$, the equilibrium E_2 is always a real saddle along the curve He^{21}. However, although the equilibrium E_1 is also a real saddle when it arises from DZ, it becomes a saddle-focus from the point DHe^{1}, which occurs at $(\varepsilon_1, \varepsilon_3) \approx (-0.25, 0.004611)$, placed between the points DHe^{21} and DZ. Precisely, the homoclinic curve H^2_1, which emerges from the Bogdanov–Takens bifurcation, ends at the point DHe^{1}. As we commented previously, an infinite sequence of homoclinic connections to E_2 arises from DHe^{1}. In Fig. 9(b)–(c) we have drawn the following two homoclinic connections, H^2_2 and H^2_3, of the mentioned sequence. Unlike what happened with the bifurcation curves of the fourth quadrant (which were organized by the degeneracies DHe^{2} and DHe^{12}), in the second quadrant the following two curves of the sequence of homoclinic connections (as well as the first curve H^2_1), now organized by the degeneracy DHe^{1}, do not end on the heteroclinic curve He^{21} (that is, they are not related to the principal heteroclinic loop).

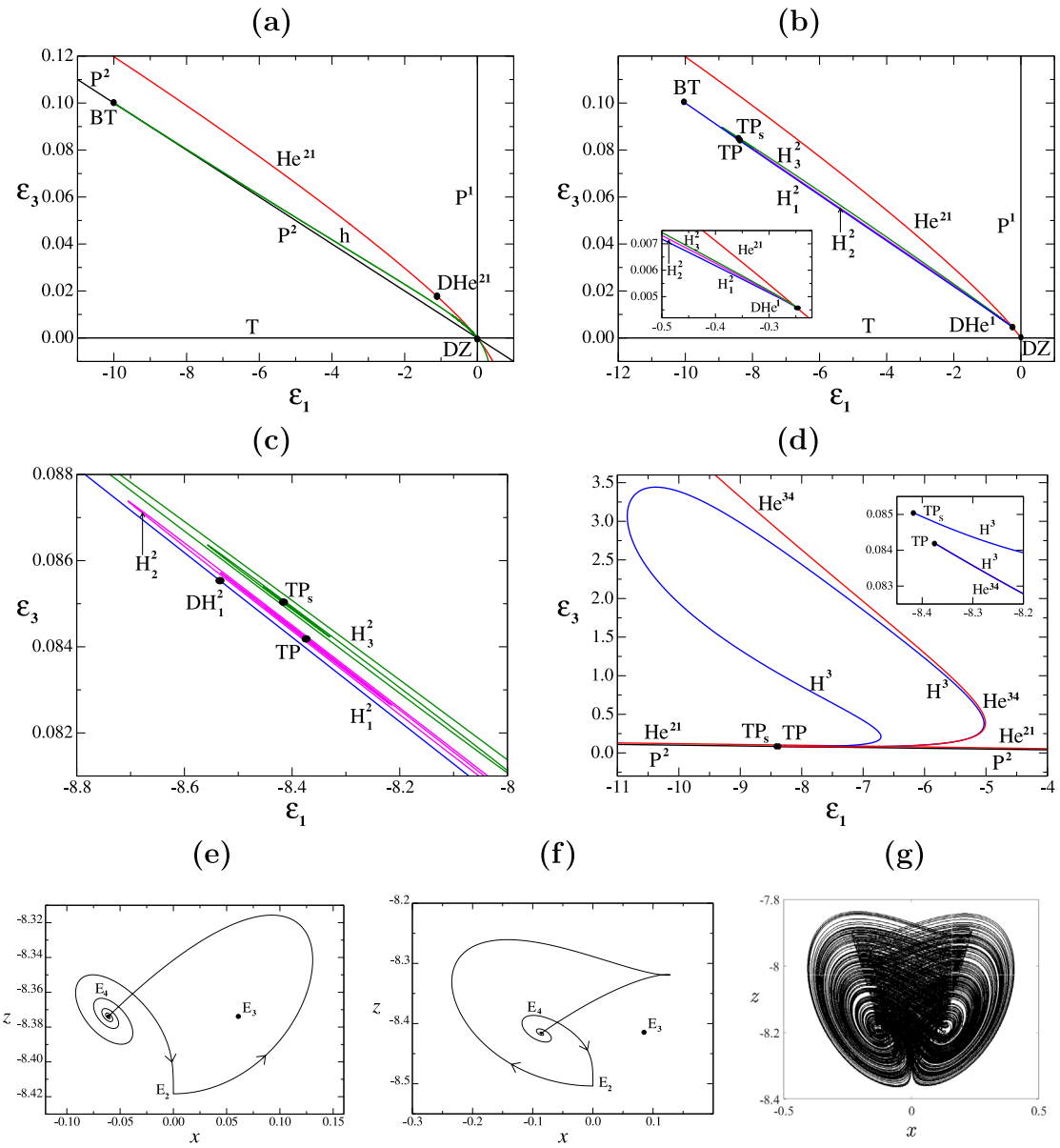

Fig. 9. For $\varepsilon_2 = -1, B = -0.1, D = 0.01$: (a)–(d) partial bifurcation set in the second quadrant of the $(\varepsilon_1, \varepsilon_3)$-plane. Projection onto the (x, z)-plane of the T-point heteroclinic loop between E_2 and the equilibria $E_{3,4}$ (note that because of the symmetry a pair of the corresponding orbits exists): (e) principal T-point when $(\varepsilon_1, \varepsilon_3) \approx (-8.3738877, 0.08418346)$; (f) secondary T-point when $(\varepsilon_1, \varepsilon_3) \approx (-8.4159326, 0.08503685)$. (g) For $(\varepsilon_1, \varepsilon_3) = (-8.2, 0.084)$, geometric Lorenz attractor with initial conditions $(x_0, y_0, z_0) = (0.2, 0, -8.2)$.

On the curve H_1^2 there exists a degenerate point DH_1^2, which occurs at $(\varepsilon_1, \varepsilon_3) \approx (-8.533961, 0.085536)$, where the condition $\delta_{E2} = 1$ (resonant eigenvalues) is fulfilled (see Fig. 9(c)). Moreover, as we can see in Fig. 9(b)–(c), the curve H_2^2 ends at the point TP, which occurs at $(\varepsilon_1, \varepsilon_3) \approx (-8.37388775, 0.08418346)$, where there exists a (principal) heteroclinic T-point loop between E_2 and $E_{3,4}$ [19,59]. Its projection on the (x, z)-plane is drawn in Fig. 9(e). As can be seen in Fig. 9(b)–(d), three curves of global connections emerge from the point TP: He^{34} (heteroclinic connections between E_3 and E_4), H^3 (homoclinic connections to E_3 and E_4) and a spiral shaped curve H_2^2 of homoclinic connections to E_2. Remark that the curves H^3 and H_3^2 end at a secondary T-point heteroclinic loop $\mathrm{TP_s}$ between E_2 and $E_{3,4}$, which occurs at $(\varepsilon_1, \varepsilon_3) \approx (-8.4159326, 0.08503685)$, whose projection on the (x, z)-plane is drawn in Fig. 9(f). In this scenario of global bifurcations the presence of chaotic motions is guaranteed [16,17]. For instance, when $(\varepsilon_1, \varepsilon_3) = (-8.2, 0.084)$ (a point placed in the range of Fig. 9(c)), the attractor obtained with initial conditions $(x_0, y_0, z_0) = (0.2, 0, -8.2)$ is represented in Fig. 9(g). Note that its shape is different from that of the other attractors drawn in Fig. 8(c)–(f).

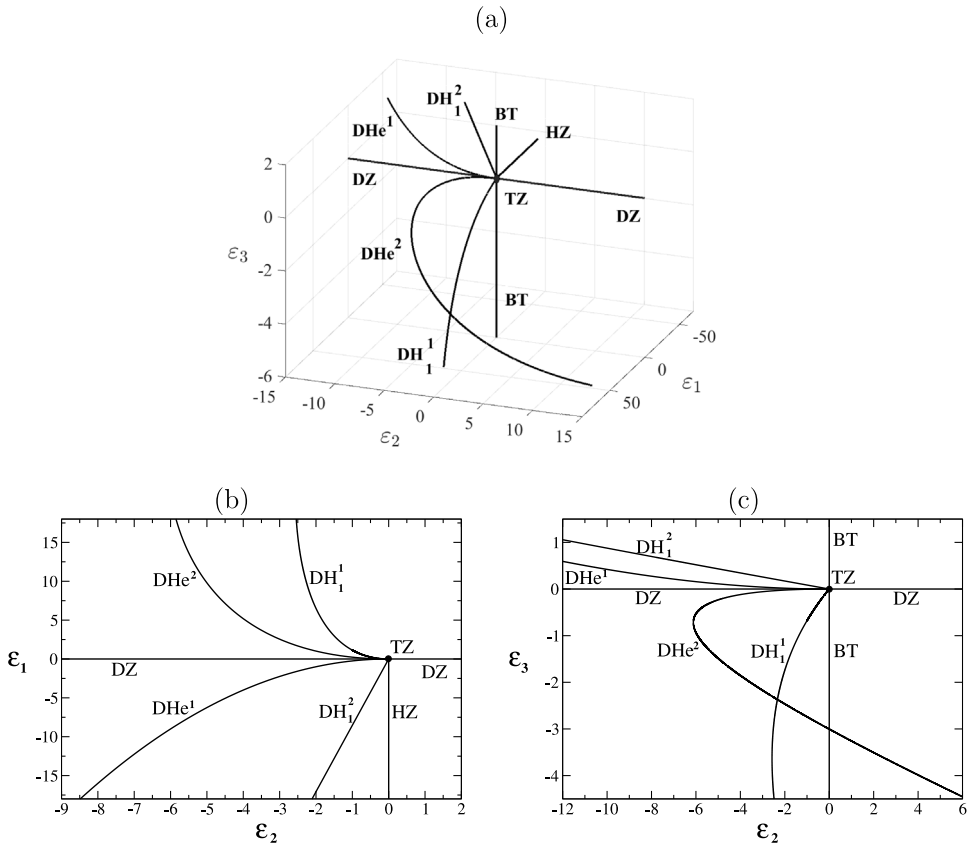

Fig. 10. Partial bifurcation set in a neighborhood of the triple-zero bifurcation TZ, for $B = -0.1$ and $D = 0.01$: (a) in the $(\varepsilon_1, \varepsilon_2, \varepsilon_3)$-space; (b) projection onto the $(\varepsilon_2, \varepsilon_1)$-plane; (c) projection onto the $(\varepsilon_2, \varepsilon_3)$-plane. Seven curves of codimension-two bifurcations appear: three are local (BT, HZ, DZ) and four are global (DHe^1, DHe^2, DH$^1_1$ and DH$^2_1$).

4.2.1. Triple-zero bifurcation

Finally, to have a global idea of the bifurcation scenario and the main organizing centers in this region of the parameter space of system (3), we have drawn in Fig. 10 a partial bifurcation set in a neighborhood of the triple-zero degeneracy TZ, when $B = -0.1$ and $D = 0.01$. The curves in the $(\varepsilon_1, \varepsilon_2, \varepsilon_3)$-space appear in Fig. 10(a), their projection onto the $(\varepsilon_2, \varepsilon_1)$-plane in Fig. 10(b) and onto the $(\varepsilon_2, \varepsilon_3)$-plane in Fig. 10(c). Specifically, we draw the loci where the following codimension-two bifurcations occur:

- BT, Bogdanov–Takens bifurcation of equilibrium E_1.
- HZ, Hopf-zero bifurcation of E_1.
- DZ, double-zero bifurcation (a double-zero eigenvalue with geometric multiplicity two) of E_1.
- DHe^1 and DHe^2, degenerate heteroclinic connections because the equilibria E_1 and E_2, respectively, change from saddle–node to saddle-focus.
- DH$^1_1$ and DH$^2_1$, degenerate homoclinic connections of E_1 and E_2 due to the existence of resonant eigenvalues $\delta_{E_1} = 1$ and $\delta_{E_2} = 1$, respectively.

Finally we emphasize that similar configurations of curves of codimension-two global bifurcations around a triple-zero degeneracy TZ have been found in previous works, both in the study of some $\mathbb{Z}_2$-symmetric control systems particularized in the Chua's equation [35] as well as in the analysis of non-symmetric electronic circuits [60].

5. Conclusions

In order to continue advancing in the analysis of the Lorenz system (and of so many other quadratic systems called Lorenz-like systems) it is necessary to combine analytical and numerical tools. Given the impossibility of studying by standard methods the triple-zero bifurcation that the equilibrium at the origin of the Lorenz system exhibits when $\sigma = -1$, $\rho = 1$, $b = 0$, in this work we carry out a partial study of system (3), an unfolding of the normal form of

the triple-zero bifurcation. We remark that several systems studied in the literature appear as particular cases for certain parameter choices [37–42].

The theoretical analysis of the double-zero bifurcation (a double-zero eigenvalue with geometric multiplicity two) has allowed to determine the different cases that may appear. For this we have established a connection between the reduced system on the corresponding two-dimensional center manifold and the planar normal form of the Hopf-zero bifurcation [44, Sect. 7.4]. For its greater interest, we have focused on the case that leads to a more complex dynamical behavior (existence of Hopf bifurcation and heteroclinic connection), and we have provided the expressions of the bifurcation curves organized by the double-zero degeneracy.

Taking as a starting point the theoretical results obtained, we have carried out a numerical study that has allowed to find bifurcations of codimension one (Hopf, transcritical, pitchfork, saddle–node of periodic orbits, heteroclinic, homoclinic), two (double-zero, Bogdanov–Takens, degenerate Hopf, degenerate heteroclinic, degenerate homoclinic, T-point) and three (degenerate double-zero, triple-zero) in the region considered of the parameter space. On the other hand, we have also found zones of existence of chaotic attractors. Various aspects of the bifurcation set of system (3) are worth studying in the future. For example, to complete the study of degeneracies that appear on the bifurcation curves and to determine the new curves that emerge from those degenerate points.

The double-zero bifurcation has allowed to find a heteroclinic connection. The degeneracies of this heteroclinic cycle are connected with the triple-zero bifurcation TZ (see Fig. 10). This codimension-three linear degeneracy deserves further study whose results can be applied to the Lorenz system.

Declaration of competing interest

The authors declare that they have no known competing financial interests or personal relationships that could have appeared to influence the work reported in this paper.

Acknowledgments

We thank the reviewers for their careful reading of the manuscript and their very constructive remarks which have helped a lot to improve the presentation of the results. This work has been partially supported by the *Ministerio de Economía y Competitividad*, Spain (project MTM2017-87915-C2-1-P, co-financed with FEDER funds), by the *Ministerio de Ciencia, Innovación y Universidades*, Spain (project PGC2018-096265-B-I00, co-financed with FEDER funds) and by the *Consejería de Economía, Innovación, Ciencia y Empleo de la Junta de Andalucía*, Spain (FQM-276, TIC-0130, UHU-1260150 and P20_01160).

Appendix A. Some useful changes of variables

The first lemma is obtained directly from the results shown in [44, Sect. 7.4]. We state it here for clarity and completeness.

Lemma A.1. *System*

$$\begin{cases} \dot{r} = arz + cr^3 + drz^2, \\ \dot{z} = -r^2 - z^2 + er^2z + fz^3, \end{cases} \tag{A.1}$$

for $a \neq 0$, by means of the change of variables

$$s = r, \quad w = z + hr^2 + iz^2, \quad d\tau = (1 + jz)^{-1}dt, \tag{A.2}$$

where

$$h = \frac{c}{a}, \quad i = \frac{d + ae + 2(a+1)c}{3a}, \quad j = \frac{ae - 2d + 2(a+1)c}{3a}, \tag{A.3}$$

is transformed into

$$\begin{cases} \dfrac{ds}{d\tau} = asw + \mathcal{O}(|s, w|^4), \\ \dfrac{dw}{d\tau} = -s^2 - w^2 + \hat{f}w^3 + \mathcal{O}(|s, w|^4), \end{cases} \tag{A.4}$$

where $\hat{f} = f - j$.

Lemma A.2. *System*

$$\begin{cases} \dot{r} = arz + cr^3z + drz^3, \\ \dot{z} = -r^2 - z^2 + er^4 + fr^2z^2 + mz^4, \end{cases} \tag{A.5}$$

for $a \neq 0, -1/2$, is orbitally equivalent to

$$\begin{cases} \dfrac{ds}{d\tau} = asw + \mathcal{O}(|s, w|^5), \\ \dfrac{dw}{d\tau} = -s^2 - w^2 + \mathcal{O}(|s, w|^5), \end{cases} \tag{A.6}$$

by means of the change of variables

$$s = r(1 + gr^2 + hz^2), \quad w = z(1 + irz + jz^2), \quad d\tau = (1 + kr^2)^{-1}dt, \tag{A.7}$$

where

$$\begin{aligned} g &= -\frac{a^2e + (a+1)c + af - 2am - d}{2a(2a+1)}, \quad h = \frac{d - am}{2}, \quad j = m, \\ i &= \frac{a(2a+5)m + (1-2a)d + ae - 2af - c}{2(2a+1)}, \quad k = \frac{ae - am - c + d}{2a}, \end{aligned} \tag{A.8}$$

Lemma A.3. *System*

$$\begin{cases} \dot{r} = arz + cr^5 + dr^3z^2 + erz^4, \\ \dot{z} = -r^2 - z^2 + fr^4z + gr^2z^3 + hz^5, \end{cases} \tag{A.9}$$

for $a \neq 0$, is orbitally equivalent to

$$\begin{cases} \dfrac{ds}{d\tau} = asw + \mathcal{O}(|s, w|^6), \\ \dfrac{dw}{d\tau} = -s^2 - w^2 + \hat{h}w^5 + \mathcal{O}(|s, w|^6), \end{cases} \tag{A.10}$$

where

$$\hat{h} = h + \frac{2(1 - 4a^2)c - 2(a+1)d + 2e - 3ag + a(1-2a)f}{5a}.$$

Appendix B. Hopf bifurcations of the nontrivial equilibria

In this appendix we analyze the Hopf bifurcations of the nontrivial equilibria $E_{3,4}$ and E_2 of system (3). The results obtained, valid for any value of ε_1, ε_2 and ε_3, will be useful in the numerical study carried out in Section 4.

B.1. Hopf bifurcation of the equilibria $E_{3,4}$

Due to the symmetry, we will only consider in our study one of these equilibria, namely $E_3 = (\sqrt{-\varepsilon_1(\varepsilon_3 + D\varepsilon_1)}, 0, \varepsilon_1)$, that exists when $\varepsilon_1(\varepsilon_3 + D\varepsilon_1) < 0$.

Firstly, we translate the nontrivial equilibria E_3 to the origin by means of the change

$$X = x - \sqrt{-\varepsilon_1(\varepsilon_3 + D\varepsilon_1)}, \quad Y = y, \quad Z = z - \varepsilon_1,$$

that transforms system (3) into

$$\begin{cases} \dot{X} &= Y, \\ \dot{Y} &= \xi_2 Y - \xi_1 Z - XZ + BYZ, \\ \dot{Z} &= 2\xi_1 X + \xi_3 Z + X^2 + DZ^2, \end{cases} \tag{B.1}$$

with

$$\xi_1 = \sqrt{-\varepsilon_1(\varepsilon_3 + D\varepsilon_1)}, \quad \xi_2 = \varepsilon_2 + B\varepsilon_1, \quad \xi_3 = \varepsilon_3 + 2D\varepsilon_1. \tag{B.2}$$

Therefore, the characteristic polynomial of the linearization matrix of system (B.1) at the origin is given by

$$p = \lambda^3 + p_1\lambda^2 + p_2\lambda + p_3,$$

where

$$p_1 = -(\xi_2 + \xi_3), \quad p_2 = \xi_2\xi_3, \quad p_3 = 2\xi_1^2.$$

Thus, a Hopf bifurcation of E_3 occurs when $p_1p_2 = p_3$, $p_2 > 0$, $p_1 \neq 0$, that is, when

$$\xi_1^2 = -\frac{1}{2}\xi_2\xi_3(\xi_2 + \xi_3), \quad \xi_2\xi_3 > 0, \quad \xi_2 + \xi_3 < 0, \quad \xi_2 < 0, \quad \xi_3 < 0.$$

Considering system (B.1) at the critical values where the Hopf bifurcation occurs, we perform the following linear change to put the matrix of the linear part into the corresponding canonical form

$$\begin{pmatrix} X \\ Y \\ Z \end{pmatrix} = \begin{pmatrix} 0 & 1 & 1 \\ \omega_0 & 0 & -K_1^2 \\ K_2 & K_3 & K_4 \end{pmatrix} \begin{pmatrix} u \\ v \\ w \end{pmatrix},$$

where

$$\omega_0 = \sqrt{\xi_2 \xi_3}, \quad K_1 = \sqrt{-(\xi_2 + \xi_3)}, \quad K_2 = \frac{\sqrt{2}\xi_2}{K_1}, \quad K_3 = \frac{\sqrt{2}\omega_0}{K_1}, \quad K_4 = \frac{\sqrt{2}\omega_0 K_1}{\xi_2}.$$

Thus, with this change, system (B.1) becomes

$$\begin{pmatrix} \dot{u} \\ \dot{v} \\ \dot{w} \end{pmatrix} = \begin{pmatrix} 0 & -\omega_0 & 0 \\ \omega_0 & 0 & 0 \\ 0 & 0 & -K_1^2 \end{pmatrix} \begin{pmatrix} u \\ v \\ w \end{pmatrix} + \frac{1}{C} \begin{pmatrix} A_1 u^2 + A_2 v^2 + A_3 w^2 + A_4 uv + A_5 uw + A_6 vw \\ A_7 u^2 + A_8 v^2 + A_9 w^2 + A_{10} uv + A_{11} uw + A_{12} vw \\ -A_7 u^2 - A_8 v^2 - A_9 w^2 - A_{10} uv - A_{11} uw - A_{12} vw \end{pmatrix}, \tag{B.3}$$

where

$$\begin{aligned}
C &= \xi_2 K_2 + \xi_3 K_2 + K_3 \omega_0 - K_4 \omega_0 \neq 0, \\
A_1 &= K_2 \left(K_3 \omega_0 - K_4 \omega_0 - \xi_2 K_2 - \xi_3 K_2\right), \\
A_2 &= {K_3}^2 E_2 + {K_3}^2 E_3 - {K_3}^2 + K_3 K_4 + E_2 + E_3, \\
A_3 &= -K_3 K_4 E_2 + 2 {K_4}^2 E_2 - K_3 K_4 E_3 + 2 {K_4}^2 E_3 - K_3 K_4 + {K_4}^2 + E_2 + E_3, \\
A_4 &= 2 K_2 K_3 E_2 + 2 K_2 K_3 E_3 - {K_3}^2 \omega_0 + K_3 K_4 \omega_0 - K_2 K_3 + K_2 K_4, \\
A_5 &= -K_2 K_3 E_2 + 3 K_2 K_4 E_2 - K_2 K_3 E_3 + 3 K_2 K_4 E_3 - K_3 K_4 \omega_0 \\
&\quad + {K_4}^2 \omega_0 - K_2 K_3 + K_2 K_4, \\
A_6 &= -{K_3}^2 E_2 + 3 K_3 K_4 E_2 - {K_3}^2 E_3 + 3 K_3 K_4 E_3 - {K_3}^2 + {K_4}^2 + 2 E_2 + 2 E_3, \\
A_7 &= 2 \omega_0 {K_2}^2, \\
A_8 &= \omega_0 {K_3}^2 + K_3 K_2 + \omega_0, \\
A_9 &= K_4 \xi_2 K_2 + K_4 \xi_3 K_2 + {K_4}^2 \omega_0 + K_4 K_2 + \omega_0, \\
A_{10} &= K_2 \left(3 K_3 \omega_0 + K_2\right), \\
A_{11} &= K_2 \left(\xi_2 K_2 + \xi_3 K_2 + 3 K_4 \omega_0 + K_2\right), \\
A_{12} &= K_3 \xi_2 K_2 + K_3 \xi_3 K_2 + 2 K_4 \omega_0 K_3 + K_3 K_2 + K_4 K_2 + 2 \omega_0.
\end{aligned}$$

Now, considering the second-order approximation to the center manifold

$$w = \alpha_1 u^2 + \alpha_2 uv + \alpha_3 v^2 + \cdots,$$

we obtain the reduced system up to third order on the center manifold. And, by using the recursive algorithm developed in [46], we obtain the normal form for the Hopf bifurcation to third-order (22), where the first Lyapunov coefficient is given by

$$a_1 = \frac{\sqrt{\xi_2 \xi_3} N_1}{4 \xi_2 \xi_3 (\xi_2 + \xi_3) \left({\xi_2}^2 + 6 \xi_2 \xi_3 + {\xi_3}^2\right) \left({\xi_2}^2 + 3 \xi_2 \xi_3 + {\xi_3}^2\right)}, \tag{B.4}$$

with

$$\begin{aligned}
N_1 &= 2 {\xi_2}^5 + 31 {\xi_2}^4 \xi_3 + 39 {\xi_2}^3 {\xi_3}^2 + {\xi_2}^2 {\xi_3}^3 - \xi_2 {\xi_3}^4 + 4 {\xi_2}^4 + 56 {\xi_2}^3 \xi_3 \\
&\quad + 25 {\xi_2}^2 {\xi_3}^2 - 12 \xi_2 {\xi_3}^3 - {\xi_3}^4 + 2 {\xi_2}^2 \xi_3 - 24 \xi_2 {\xi_3}^2 - 2 {\xi_3}^3.
\end{aligned}$$

Since $\xi_2 \xi_3 > 0$, we obtain that $a_1 = 0$ if, and only if, $N_1 = 0$.

In Fig. B.1 we have drawn the curve $N_1 = 0$ in the (ξ_2, ξ_3)-plane near the origin. It is a bounded curve connecting the points $(-2, 0)$ and $(0, -2)$.

In terms of the original parameters of the system, the Hopf surface of the equilibria $E_{3,4}$ is given by

$$\begin{aligned}
\varepsilon_3 &= \frac{2\varepsilon_1 - 2(B + 2D)\varepsilon_1 \varepsilon_2 - B(B + 4D)\varepsilon_1^2 - \varepsilon_2^2}{2(B\varepsilon_1 + \varepsilon_2)} \\
&\quad + \frac{\sqrt{(B\varepsilon_1 + \varepsilon_2)^4 + 4\varepsilon_1(\varepsilon_1 - 2D(B\varepsilon_1 + \varepsilon_2)\varepsilon_1 - (B\varepsilon_1 + \varepsilon_2)^2)}}{2(B\varepsilon_1 + \varepsilon_2)},
\end{aligned} \tag{B.5}$$

in the zones where the above inequalities are fulfilled.

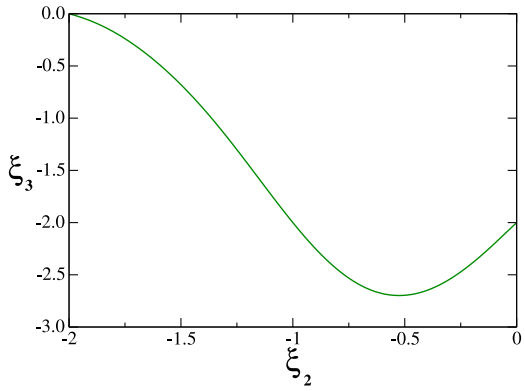

Fig. B.1. Curve $N_1 = 0$ in the (ξ_2, ξ_3)-plane in the vicinity of the origin. It corresponds to the degeneracy $a_1 = 0$ in the Hopf bifurcation of the equilibria $E_{3,4}$.

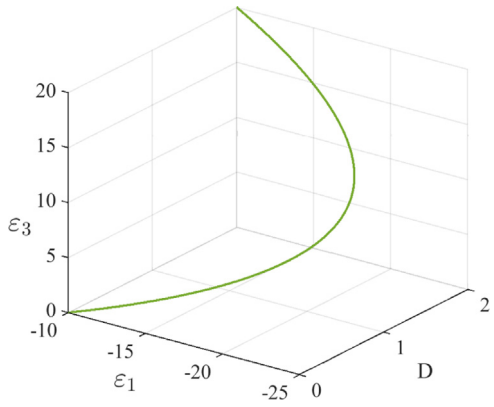

Fig. B.2. For $\varepsilon_2 = -1$, $B = -0.1$, curve on the Hopf surface where $M_1 = 0$ in the $(D, \varepsilon_1, \varepsilon_3)$-space. It corresponds to the degeneracy $a_1 = 0$ in the Hopf bifurcation of equilibrium E_2.

B.2. Hopf bifurcation of the equilibrium E_2

Now we consider the equilibrium $E_2 = (0, 0, -\varepsilon_3/D)$. According to Section 2, it exhibits a Hopf bifurcation when $B\varepsilon_3 = D\varepsilon_2$, if $\varepsilon_1 + \varepsilon_3/D < 0$ and $\varepsilon_3 \neq 0$. Repeating the previous calculations we obtain that the first Lyapunov coefficient, in terms of the original parameters of the system, is given by

$$a_1 = \frac{B^2 M_1}{8\sqrt{-\frac{B\varepsilon_1+\varepsilon_2}{B}}\, D\, \varepsilon_2 \left(4B^2\varepsilon_1 + 4B\varepsilon_2 - D^2 {\varepsilon_2}^2\right)}, \tag{B.6}$$

with

$$M_1 = 8B^2\varepsilon_1 + 8B\varepsilon_2 - D^2{\varepsilon_2}^2 - 2D\varepsilon_2.$$

If $B \neq 0$, we obtain that $a_1 = 0$ if, and only if, $M_1 = 0$.

For $\varepsilon_2 = -1$ and $B = -0.1 < 0$, in Fig. B.2 we have drawn, in the $(D, \varepsilon_1, \varepsilon_3)$-space, the curve on the Hopf surface where $M_1 = 0$. This curve exists between the points $(0, -10, 0)$ (where a triple-zero bifurcation in a continuum of equilibria occurs) and $(2, -10, 20)$ (that corresponds to a degenerate Bogdanov–Takens bifurcation) [43]. Also, if we set a value $D \in (0, 2)$, there is a unique degeneracy $a_1 = 0$ on the Hopf curve of E_2 when $\varepsilon_1 < -10$, and there are no degenerations if $D < 0$.

References

[1] Lorenz EN. Deterministic non-periodic flows. J Atmospheric Sci 1963;20:130–41. http://dx.doi.org/10.1175/1520-0469(1963)020<0130:DNF>2.0.CO;2.

[2] Sparrow C. The Lorenz equation: bifurcations, chaos and strange attractors. New York: Springer; 1982, http://dx.doi.org/10.1007/978-1-4612-5767-7.

[3] Haken H. Analogy between higher instabilities in fluids and lasers. Phys Lett A 1975;53:77–8. http://dx.doi.org/10.1016/0375-9601(75)90353-9.
[4] Knobloch E. Chaos in the segmented disc dynamo. Phys Lett A 1981;82:439–40. http://dx.doi.org/10.1016/0375-9601(81)90274-7.
[5] Gorman M, Widmann PJ, Robbins KA. Nonlinear dynamics of a convection loop: a quantitative comparison of experiment with theory. Physica D 1986;19:255–67. http://dx.doi.org/10.1016/0167-2789(86)90022-9.
[6] Elgin JN, Molina-Garza JB. Traveling wave solutions of the Maxwell–Bloch equations. Phys Rev A 1987;35:3986–8. http://dx.doi.org/10.1103/PhysRevA.35.3986.
[7] Knobloch E, Proctor MRE, Weiss NO. Heteroclinic bifurcations in a simple model of double-diffusive convection. J Fluid Mech 1992;239:273–92. http://dx.doi.org/10.1017/S0022112092004403.
[8] Cuomo KM, Oppenheim AV. Circuit implementation of synchronized chaos with applications to communications. Phys Rev Lett 1993;71:65–8. http://dx.doi.org/10.1103/PhysRevLett.71.65.
[9] Poland D. Cooperative catalysis and chemical chaos: a chemical model for the Lorenz equations. Physica D 1993;65:86–99. http://dx.doi.org/10.1016/0167-2789(93)90006-M.
[10] Hemati N. Strange attractors in brushless DC motors. IEEE T Circuits-I 1994;41:40–5. http://dx.doi.org/10.1109/81.260218.
[11] Alexeev I. Lorenz system in the thermodynamic modelling of leukaemia malignancy. Med Hypotheses 2017;102:150–5. http://dx.doi.org/10.1016/j.mehy.2017.03.027.
[12] Tucker W. The Lorenz attractor exists. C R Acad Sci 1999;328:1197–202. http://dx.doi.org/10.1016/S0764-4442(99)80439-X.
[13] Osinga HM, Krauskopf B. Visualizing the structure of chaos in the Lorenz system. Comput Graph 2002;26:815–23. http://dx.doi.org/10.1016/S0097-8493(02)00136-X.
[14] Barrio R, Serrano S. Bounds for the chaotic region in the Lorenz model. Physica D 2009;238:1615–24. http://dx.doi.org/10.1016/j.physd.2009.04.019.
[15] Yajima T, Nagahama H. Tangent bundle viewpoint of the Lorenz system and its chaotic behavior. Phys Lett A 2010;374:1315–9. http://dx.doi.org/10.1016/j.physleta.2010.01.025.
[16] Barrio R, Blesa F, Serrano S. Global organization of spiral structures in biparameter space of dissipative systems with Shilnikov saddle-foci. Phys Rev E 2011;84:035201. http://dx.doi.org/10.1103/PhysRevE.84.035201.
[17] Barrio R, Shilnikov AL, Shilnikov LP. Kneadings, symbolic dynamics and painting Lorenz chaos. Int J Bifurcation Chaos 2012;22:1230016. http://dx.doi.org/10.1142/S0218127412300169.
[18] Leonov GA, Kuznetsov NV, Korzhemanova NA, Kusakin DV. Lyapunov dimension formula for the global attractor of the Lorenz system. Commun Nonlinear Sci Numer Simul 2016;41:84–103. http://dx.doi.org/10.1016/j.cnsns.2016.04.032.
[19] Glendinning P, Sparrow C. T-points: a codimension two heteroclinic bifurcation. J Stat Phys 1986;43:479–88. http://dx.doi.org/10.1007/BF01020649.
[20] Algaba A, Fernández-Sánchez F, Merino M, Rodríguez-Luis AJ. Analysis of the T-point-Hopf bifurcation in the Lorenz system. Commun Nonlinear Sci Numer Simul 2015;22:676–91. http://dx.doi.org/10.1016/j.cnsns.2014.09.025.
[21] Creaser JL, Krauskopf B, Osinga HM. α-Flips and T-points in the Lorenz system. Nonlinearity 2015;28:R39–65. http://dx.doi.org/10.1088/0951-7715/28/3/R39.
[22] Doedel EJ, Krauskopf B, Osinga HM. Global bifurcations of the Lorenz manifold. Nonlinearity 2006;19:2947–72. http://dx.doi.org/10.1088/0951-7715/19/12/013.
[23] Doedel EJ, Krauskopf B, Osinga HM. Global invariant manifolds in the transition to preturbulence in the Lorenz system. Indag Math 2011;22:222–40. http://dx.doi.org/10.1016/j.indag.2011.10.007.
[24] Doedel EJ, Krauskopf B, Osinga HM. Global organization of phase space in the transition to chaos in the Lorenz system. Nonlinearity 2015;28:R113–39. http://dx.doi.org/10.1088/0951-7715/28/11/R113.
[25] Llibre J, Zhang X. Invariant algebraic surfaces of the Lorenz system. J Math Phys 2002;43:1622–45. http://dx.doi.org/10.1063/1.1435078.
[26] Llibre J, Messias M, da Silva PR. Global dynamics of the Lorenz system with invariant algebraic surfaces. Int J Bifurcation Chaos 2010;20:3137–55. http://dx.doi.org/10.1142/S0218127410027593.
[27] Algaba A, Gamero E, Merino M, Rodríguez-Luis AJ. Resonances of periodic orbits in the Lorenz system. Nonlinear Dyn 2016;84:2111–36. http://dx.doi.org/10.1007/s11071-016-2632-5.
[28] Algaba A, Merino M, Rodríguez-Luis AJ. Superluminal periodic orbits in the Lorenz system. Commun Nonlinear Sci Numer Simul 2016;39:220–32. http://dx.doi.org/10.1016/j.cnsns.2016.03.004.
[29] Algaba A, Fernández-Sánchez F, Merino M, Rodríguez-Luis AJ. Centers on center manifolds in the Lorenz, Chen and Lü systems. Commun Nonlinear Sci Numer Simul 2014;19:772–5. http://dx.doi.org/10.1016/j.cnsns.2013.08.003.
[30] Algaba A, Domínguez-Moreno MC, Merino M, Rodríguez-Luis AJ. Study of the Hopf bifurcation in the Lorenz, Chen and Lü systems. Nonlinear Dyn 2015;79:885–902. http://dx.doi.org/10.1007/s11071-014-1709-2.
[31] Algaba A, Domínguez-Moreno MC, Merino M, Rodríguez-Luis AJ. Takens–Bogdanov bifurcations of equilibria and periodic orbits in the Lorenz system. Commun Nonlinear Sci Numer Simul 2016;30:328–43. http://dx.doi.org/10.1016/j.cnsns.2015.06.034.
[32] Algaba A, Domínguez-Moreno MC, Merino M, Rodríguez-Luis AJ. A review on some bifurcations in the Lorenz system. In: Carmona V, et al., editors. Nonlinear systems, vol. 1. Mathematical theory and computational methods. Cham: Springer; 2018, p. 3–36. http://dx.doi.org/10.1007/978-3-319-66766-9_1.
[33] Gamero E. On the normal form of the triple-zero degeneracy with geometric multiplicity two. Dynam Cont Dis Ser A 2001;8:531–50.
[34] Freire E, Gamero E, Rodríguez-Luis AJ, Algaba A. A note on the triple-zero linear degeneracy: Normal forms, dynamical and bifurcation behaviors of an unfolding. Int J Bifurcation Chaos 2002;12:2799–820. http://dx.doi.org/10.1142/S0218127402006175.
[35] Algaba A, Merino M, Freire E, Gamero E, Rodríguez-Luis AJ. Some results on Chua's equation near a triple-zero linear degeneracy. Int J Bifurcation Chaos 2003;13:583–608. http://dx.doi.org/10.1142/S0218127403006741.
[36] Gamero E, Freire E, Rodríguez-Luis AJ, Ponce E, Algaba A. Hypernormal form calculation for triple-zero degeneracies. Bull Belg Math Soc Simon Stevin 1999;6:357–68. http://dx.doi.org/10.36045/bbms/1103065855.
[37] Shimizu T, Morioka N. On the bifurcation of a symmetric limit cycle to an asymmetric one in a simple model. Phys Lett A 1980;76:201–4. http://dx.doi.org/10.1016/0375-9601(80)90466-1.
[38] Shil'nikov AL. On bifurcations of the Lorenz attractor in the Shimizu-Morioka model. Physica D 1993;62:338–46. http://dx.doi.org/10.1016/0167-2789(93)90292-9.
[39] Rucklidge AM. Chaos in a low-order model of magnetoconvection. Physica D 1993;62:323–37. http://dx.doi.org/10.1016/0167-2789(93)90291-8.
[40] Liu C, Liu T, Liu L, Liu K. A new chaotic attractor. Chaos Solitons Fractals 2004;22:1031–8. http://dx.doi.org/10.1016/j.chaos.2004.02.060.
[41] Mello LF, Messias M, Braga DC. Bifurcation analysis of a new Lorenz-like chaotic system. Chaos Solitons Fractals 2008;37:1224–55. http://dx.doi.org/10.1016/j.chaos.2007.11.008.
[42] Kokubu H, Roussarie R. Existence of a singulary degenerate heteroclinic cycle in the Lorenz system and its dynamical consequences: Part I. J Dyn Differ Equ 2004;16:513–57. http://dx.doi.org/10.1007/s10884-004-4290-4.

[43] Algaba A, Domínguez-Moreno MC, Merino M, Rodríguez-Luis AJ. A degenerate Takens–Bogdanov bifurcation in a normal form of Lorenz's equations. In: Lacarbonara W, et al., editors. Advances in Nonlinear Dynamics. Proceedings of the Second International Nonlinear Dynamics Conference (NODYCON 2021), vol. 1. Cham: Springer; 2022, p. 699–709. http://dx.doi.org/10.1007/978-3-030-81162-4_60.
[44] Guckenheimer J, Holmes PJ. Nonlinear oscillations, dynamical systems, and bifurcations of vector fields. New York: Springer; 1983, http://dx.doi.org/10.1007/978-1-4612-1140-2.
[45] Wiggins S. Introduction to applied dynamical systems and chaos. New York: Springer; 2003, http://dx.doi.org/10.1007/b97481.
[46] Gamero E, Freire E, Ponce E. Normal forms for planar systems with nilpotent linear part. In: Seydel R, et al., editors. Bifurcation and chaos: analysis, algorithms, applications. International Series of Numerical Mathematics, vol. 97, Basel: Birkhäuser; 1991, p. 123–7. http://dx.doi.org/10.1007/978-3-0348-7004-7_14.
[47] Keener JP. Infinite period bifurcation and global bifurcation branches. SIAM J Appl Math 1981;41:127–44. http://dx.doi.org/10.1137/0141010.
[48] Chow SN, Li C, Wang D. Normal forms and bifurcation of planar vector fields. Cambridge: Cambridge University Press; 1994, http://dx.doi.org/10.1017/CBO9780511665639.
[49] Qin BW, Chung KW, Algaba A, Rodríguez-Luis AJ. High-order approximation of heteroclinic bifurcations in truncated 2D-normal forms for the generic cases of Hopf-zero and non-resonant double Hopf singularities. SIAM J Appl Dynam Syst 2021;20:403–37. http://dx.doi.org/10.1137/0141010.
[50] Algaba A, Chung KW, Qin BW, Rodríguez-Luis AJ. A nonlinear time transformation method to compute all the coefficients for the homoclinic bifurcation in the quadratic Takens–Bogdanov normal form. Nonlinear Dyn 2019;97:979–90. http://dx.doi.org/10.1007/s11071-019-05025-2.
[51] Algaba A, Chung KW, Qin BW, Rodríguez-Luis AJ. Computation of all the coefficients for the global connections in the $\mathbb{Z}_2$-symmetric Takens–Bogdanov normal forms. Commun Nonlinear Sci Numer Simul 2020;81:105012. http://dx.doi.org/10.1016/j.cnsns.2019.105012.
[52] Qin BW, Chung KW, Algaba A, Rodríguez-Luis AJ. High-order analysis of global bifurcations in a codimension-three Takens–Bogdanov singularity in reversible systems. Int J Bifurcation Chaos 2020;30:2050017. http://dx.doi.org/10.1142/S0218127420500170.
[53] Qin BW, Chung KW, Algaba A, Rodríguez-Luis AJ. Analytical approximation of cuspidal loops using a nonlinear time transformation method. Appl Math Comput 2020;373:125042. http://dx.doi.org/10.1016/j.amc.2020.125042.
[54] Qin BW, Chung KW. Personal communication (2019).
[55] Doedel EJ, Champneys AR, Dercole F, Fairgrieve T, Kuznetsov Y, Oldeman BE, Paffenroth R, Sandstede B, Wang X, Zhang C. Auto07-P: Continuation and bifurcation software for ordinary differential equations (with HomCont). Technical report, Concordia University; 2012.
[56] Krupa M, Melbourne I. Asymptotic stability of heteroclinic cycles in systems with symmetry. Ergod Theor Dyn Syst 1995;15:121–47. http://dx.doi.org/10.1017/S0143385700008270.
[57] Krupa M, Melbourne I. Asymptotic stability of heteroclinic cycles in systems with symmetry, II. P Roy Soc Edinb A 2004;134:1177–97. http://dx.doi.org/10.1017/S0308210500003693.
[58] Geng F, Xu Y. Bifurcations of heteroclinic loop accompanied by pitchfork bifurcation. Nonlinear Dyn 2012;70:1645–55. http://dx.doi.org/10.1007/s11071-012-0563-3.
[59] Fernández-Sánchez F, Freire E, Rodríguez-Luis AJ. T-points in a $\mathbb{Z}_2$-symmetric electronic oscillator. (I) Analysis. Nonlinear Dynam 2002;28:53–69. http://dx.doi.org/10.1023/A:1014917324652.
[60] Algaba A, Merino M, García C, Reyes M. Degenerate global bifurcations in a simple circuit. Int J Pure Appl Math 2009;57:265–78.